

Master's thesis

DOD INKJET PRINTING OF PHARMACEUTICAL LIQUIDS FOR APPLICATION IN PERSONALIZED MEDICINE

Nina Schrödl

Institute of Fluid Mechanics and Heat Transfer

University of Technology Graz

Head of department: O. Univ.-Prof. Dipl.-Ing. Dr.-Ing. habil Günter Brenn



Advisor: O. Univ.-Prof. Dipl.-Ing. Dr.-Ing. habil Günter Brenn

Graz, November 2012

In cooperation with:

RCPE Research Center Pharmaceutical Engineering GmbH



STATUTORY DECLARATION

I declare that I have authored this thesis independently, that I have not used other than the declared sources / resources, and that I have explicitly marked all material which has been quoted either literally or by content from the used sources.

.....

date

.....

(signature)

ABSTRACT

In this work inkjet printing is investigated as a dosing method for liquid pharmaceutical preparations. Printing of pharmaceutical solutions, e.g. on edible paper substrates, allows the application of individualized doses and could therefore be a promising method in personalized medicine.

Three vitamins (pyridoxine hydrochloride, cyanocobalamin and folic acid) are dissolved or suspended in a carrier fluid and tested for their ejectability in a commercially available drop-on-demand droplet generator. The different stages of drop formation are observed and droplet diameter and velocity are measured as functions of the control parameters of the droplet generator (dispensing frequency, pulse width and pulse amplitude). Based on these data, correlations for the prediction of droplet diameter and velocity are determined.

In addition, the dispensing of pharmaceutical barrier coatings, which are usually used in tablet coating, are tested. The accuracy of the dispensing process is investigated by weighing droplet portions and comparing the mass to optical measurements. Drop impact tests on glass and four paper substrates are conducted to determine whether an ejected droplet is deposited or splashed on a substrate. The release of a printed substance from paper is investigated by means of dissolution tests.

Stable drop formation is achieved for all vitamin solutions and suspensions with the exception of pyridoxine hydrochloride. Diluted coating solutions are ejectable, but the operating parameters change over time and the droplet generator is prone to clogging. The drop impact tests showed that droplets are deposited, not splashed on the test substrates. The dissolution experiments revealed that the test substances are released within the first five minutes from the paper carrier.

The correlation models were good with R^2 values of 0.9933 for the drop diameter and 0.9667 for the drop velocity.

ACKNOWLEDGEMENTS

First of all, I would like to express my deepest gratitude to my advisor O. Univ.-Prof. Dipl. Ing. Dr.-Ing. habil Günter Brenn who gave me the opportunity to write my master's thesis at the Institute of Fluid Dynamics and Heat Transfer. He introduced me to a fascinating field of research and I am very grateful for his advice and patience with me.

Also, I would like to acknowledge Tania Garcia for taking the time to introduce me to laboratory equipment and helping me with data analysis in Matlab.

I would also like to thank my supervisor at the Research Center for Pharmaceutical Engineering Dipl.-Ing. Dr. Christine Voura for her constant support and confidence in my work.

I would also like to show my gratitude to my coworkers at the RCPE. My sincere thanks go to Michael Gruber, BSc for performing the HPLC analysis and Mag. Daniela Strohmeier for producing the folic acid suspensions used in this study. Furthermore I would like to thank Bernhard Sirnik for designing and building the moveable sample stage as well as Georg Neubauer and Thomas Taucher for their technical support.

Finally I would like to thank my family. I am indebted to my parents for their unconditional support during my studies and especially to my partner Robert for his love and understanding. Without them, none of this would have been possible.

TABLE OF CONTENTS

| | |
|---|------|
| Nomenclature..... | VIII |
| 1 Introduction..... | 1 |
| 1.1 Personalized medicine | 1 |
| 1.2 Motivation and approach | 1 |
| 2 Fundamentals..... | 3 |
| 2.1 DOD inkjet printing | 3 |
| 2.1.1 Piezoelectrically driven Inkjet device | 3 |
| 2.1.2 Hydrodynamics of droplet generation | 5 |
| 2.2 Formulation requirements..... | 7 |
| 2.3 Pharmaceutical ingredients studied | 8 |
| 2.3.1 Vitamin B6 (Pyridoxine hydrochloride) | 8 |
| 2.3.2 Vitamin B9 (Folic acid) | 9 |
| 2.3.3 Vitamin B12 (Cyanocobalamin) | 10 |
| 2.4 Coatings..... | 3 |
| 3 Materials and Methods | 14 |
| 3.1 Materials | 14 |
| 3.1.1 Chemicals..... | 14 |
| 3.1.2 Solvents and solvent mixtures..... | 14 |
| 3.1.3 Solutions | 15 |
| 3.1.4 Suspensions | 15 |
| 3.1.5 Polymer coatings | 16 |
| 3.1.6 Paper..... | 17 |
| 3.2 Experimental setup and image processing..... | 17 |
| 3.2.1 Setup for drop diameter and velocity measurements | 17 |
| 3.2.2 Setup for droplet mass measurements..... | 18 |
| 3.2.3 Setup for impact behavior tests | 19 |
| 3.3 Methods..... | 20 |
| 3.3.1 Physical characterization of the liquids..... | 20 |
| 3.3.2 Dimensional analysis | 22 |

| | | |
|-------|---|----|
| 3.3.3 | Droplet gravimetry | 22 |
| 3.3.4 | Dissolution testing | 24 |
| 4 | Physical Processes Investigated | 25 |
| 4.1 | Droplet formation process..... | 25 |
| 4.2 | Droplet diameter and velocity..... | 25 |
| 4.3 | Drop impact | 26 |
| 5 | Results and Discussion..... | 29 |
| 5.1 | Liquid properties..... | 29 |
| 5.1.1 | Rheological properties..... | 30 |
| 5.1.2 | Contact angle..... | 33 |
| 5.2 | Drop-on-demand droplet ejection | 35 |
| 5.2.1 | Vitamin solutions..... | 35 |
| 5.2.2 | Polymer coatings | 37 |
| 5.2.3 | Folic acid suspensions..... | 40 |
| 5.3 | Drop formation process..... | 43 |
| 5.4 | Dosing accuracy | 50 |
| 5.5 | Drop impact and spreading | 53 |
| 5.6 | Dissolution testing | 59 |
| 5.7 | Dimensional analysis and correlation model..... | 63 |
| 5.7.1 | Correlation for the drop diameter..... | 65 |
| 5.7.2 | Correlation for the drop velocity..... | 66 |
| 6 | Summary and Conclusions | 68 |
| 6.1 | Summary..... | 68 |
| 6.2 | Concluding remarks | 69 |
| 7 | References..... | 72 |

NOMENCLATURE

Abbreviations

| | |
|---------------------|---|
| H ₂ O dd | bi-distilled water |
| EtOH | ethanol |
| PG | propylene glycol (propane-1,2-diol) |
| PEG | polyethylene glycol (poly (ethylene oxide)) |
| B2 | vitamin B2 (riboflavin) |
| B6 | vitamin B6 (pyridoxine HCl) |
| B12 | vitamin B12 (cyanocobalamin) |
| FA | folic acid |
| de-ion | de-ionized |
| NaOH | sodium hydroxide |
| API | active pharmaceutical ingredient |
| CaCO ₃ | calcium carbonate |
| TiO ₂ | titanium dioxide |
| iPrOH | isopropyl alcohol |
| rt | room temperature |
| MEK | methyl ethyl ketone |
| T20 | tween 20 (polysorbate 20) |
| Gly | glycerol |

Physical quantities

| | | |
|------------|--|----------------------------|
| Re | Reynolds number ($\rho d_d u / \mu$) | [1] |
| We | Weber number ($\rho d_d u^2 / \sigma$) | [1] |
| Oh | Ohnesorge number ($\mu / (\rho \sigma d_d)^{1/2}$) | [1] |
| d_d | droplet diameter | [m] |
| u | droplet velocity | [m/s] |
| ρ | density | [kg/m ³] |
| μ | dynamic viscosity | [kg/(ms)] |
| σ | surface tension | [kg/s ²] |
| ΔU | voltage amplitude | [V] |
| f | frequency | [s ⁻¹] |
| τ | pulse width | [s] |
| β | piezoelectric constant | [= $3 \cdot 10^{-10}$ m/V] |
| d | capillary diameter | [= $8 \cdot 10^{-4}$ m] |

1 INTRODUCTION

1.1 PERSONALIZED MEDICINE

Personalized medicine is a medical concept that is aimed at an individualized treatment of the patient. It takes the patient's genomic and family background, as well as other aspects like gender, age and size into consideration and tries to optimize the patient's treatment.

1.2 MOTIVATION AND APPROACH

The objective of this work was to investigate inkjet printing for a possible application in personalized medicine. Drugs could be printed on edible paper substrates that are subsequently rolled up and inserted into a standard hard gelatin capsule for oral administration.

Especially for drugs administered in very low doses, inkjet printing could be an excellent dosing method. Inkjet printheads can generate microdroplets in the picoliter range and would therefore allow for precise dosing of liquid formulations. Inkjet technology could provide a useful method for printing drugs on demand in individualized doses tailored to the needs of the patient. Furthermore, the application of multiple active pharmaceutical ingredients on one substrate could reduce the amount of tablets or capsules a patient would have to take. In addition, printing of medicines could be useful for clinical trial studies, because it could shorten the usual pre-formulation process.

The approach was to develop a chemically stable liquid formulation of three test substances (vitamin B6, B12 and folic acid) suitable for drop-on-demand droplet ejection. These liquids were characterized for their physical properties and tested in a commercially available droplet ejector. DOD drop formation was studied to determine optimum fluid properties and drive settings for the droplet generator. Droplet diameter and velocity were measured and correlation models were developed based on these measurements to predict droplet size and ejection velocity.

Selected liquids that exhibited good ejectability were then printed on paper carriers and subjected to dissolution testing to determine dosing accuracy of the used system and substance release from the paper substrate. In addition, drop impact tests on paper

substrates were carried out to determine if microdroplets would splash on impact and distribute the test substance in an unfavorable way. The deposition of polymeric protective coatings with an inkjet printhead was also tested.

2 FUNDAMENTALS

2.1 DOD INKJET PRINTING

DOD inkjet printing is one of the most versatile technologies that allows for many applications outside its traditional use. It has been successfully used for the deposition of bacteria [1] and various other biological samples [2][3][4]. It has proven useful for analytical purposes like, for example, the dosing of small volumes for UPLC analysis [5] or the injection of droplets for serial crystallography of proteins [6]. It has been further applied in manufacturing of polymer LEDs [7][8] and LCDs [9], in solid freeform fabrication [10] and the printing of metal or metal oxide suspensions for the fabrication of electronic components [11][12][13].

2.1.1 PIEZOELECTRICALLY DRIVEN INKJET DEVICE

The piezoelectrically driven droplet generator used in this study consists of a glass capillary with defined diameter that tapers on one end to a fine nozzle tip with an aperture of 100 μm in diameter. The capillary is partly enclosed by a cylindrical piezoelectric element that transduces electrical impulses into mechanical motion. This creates a pressure wave that is able to push a liquid portion through the nozzle aperture. Ideally, a stable droplet is formed that separates from the liquid filament pushed through the capillary orifice, and the rest liquid is retracted into the nozzle.

On the other end, the capillary is connected to a fluid reservoir via a PTFE hose.

Figure 1 shows a schematic drawing of a squeeze-mode tubular reservoir droplet ejector, similar to the one used in this study.

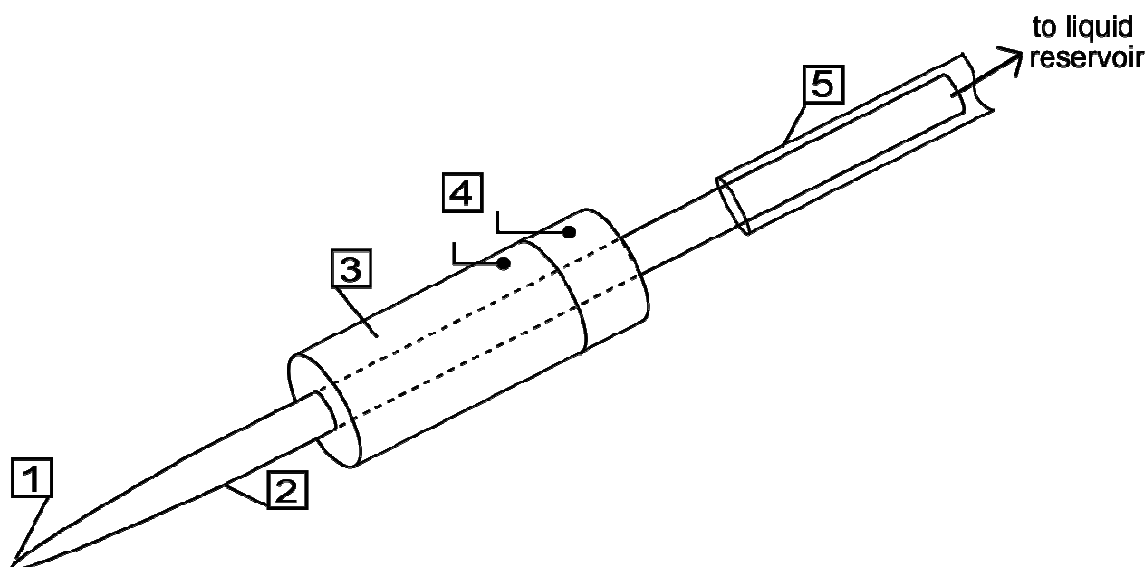


Figure 1: Schematic diagram of a piezoelectrically driven microdrop ejector. (1) Nozzle, (2) glass capillary, (3) piezoelectric transducer, (4) voltage supply, (5) PTFE hose.

For dispensing high viscosity liquids, nozzle and fluid reservoir can be heated up to 80°C and 100°C, respectively. The droplet generator can be operated in a continuous or a burst mode. In continuous mode, a stream of droplets is produced at a fixed ejection rate, while the burst mode allows for the dispensing of a preset number of droplets ranging from 1 to 10000 droplets. A negative internal pressure (holding pressure) can be applied to the capillary to avoid the fluid dripping when the capillary forces are not strong enough to keep the liquid inside the nozzle. In addition, a positive pressure can be applied to the liquid reservoir in order to fill or purge the capillary.

The piezoelectric element is actuated by a dispenser driver unit controlled via the GUI software provided by the manufacturer. Pulse width (5 – 255 μs), driving amplitude (30 – 255 V) and ejection frequency (1Hz - 6 kHz) of the actuation signal can be adjusted to optimum drive settings for drop formation.

Figure 2 displays a typical rectangular driving signal. In this example the drive amplitude is set to 100 V, and the pulse width is 30 μs . Rise and falling time of the control impulse are unknown and specific to the used electronic waveform generator that does not allow for a change of the pulse shape.

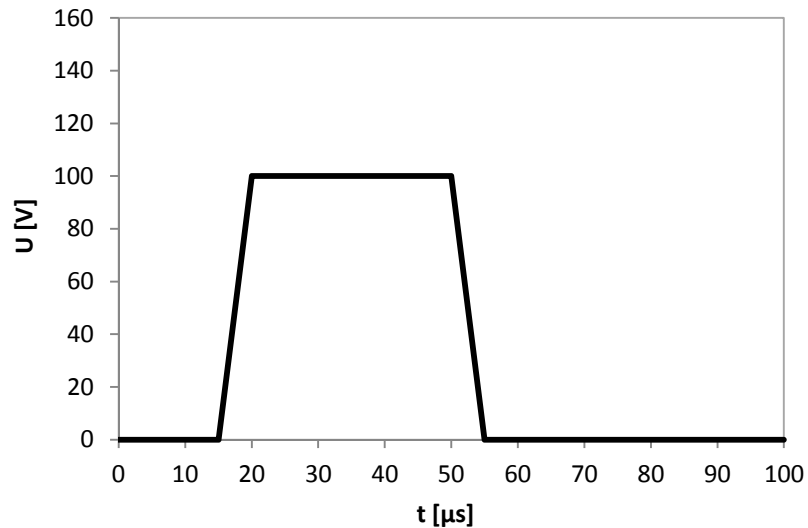


Figure 2: Pulse shape of a typical actuation signal.

The driving amplitude determines the amount of pressure in the capillary. It influences the droplet velocity and, to a certain extent, also the droplet size. Excess voltage can lead to satellite or spray formation and to air entrapment in the nozzle [14]. The pulse width determines how long the pressure is applied to the liquid. An increase in pulse width usually results in an increase of droplet size. Adjusting the pulse width can also improve directional stability of the ejected droplets.

The ejection rate or dispensing frequency defines the number of impulses produced and thus determines the number of droplets ejected per time unit. Usually there is a maximum ejection rate that depends on the fluid properties.

2.1.2 HYDRODYNAMICS OF DROPLET GENERATION

Piezoelectric droplet ejectors generate microdroplets by changing the volume of the fluid reservoir and thus ejecting fluid from the nozzle orifice. When an electrical impulse is applied to the actuator, a radial displacement of the capillary is induced. An increase in voltage can either expand (negative control) or contract (positive control) the piezoelectric actuator. In case of positive control, the actuator contracts when voltage is applied and creates a positive pressure pulse in the capillary that pushes liquid out of the nozzle aperture. After the voltage goes back to zero, the actuator expands again. Negative control means that the actuator expands when voltage is applied, thus creating a negative pressure

inside the droplet generator. When the driving signal is stopped, the actuator contracts and creates yet another positive pressure wave.

Bogy and Talke analyzed and described wave propagation phenomena in conjunction with drop-on-demand drop formation [15]. They used piezoelectric droplet generators with cylindrical actuator geometry and different cavity lengths (L). Cavity refers to the inside of the glass capillary of the droplet ejector. The applied drive signal was a rectangular impulse. Based on theoretical considerations and experimental observations they concluded that DOD drop formation is caused by propagation and reflection of acoustic waves in the liquid chamber. Figure 3 shows a graphical representation of the acoustic phenomena that occur when the piezoelectric element is actuated.

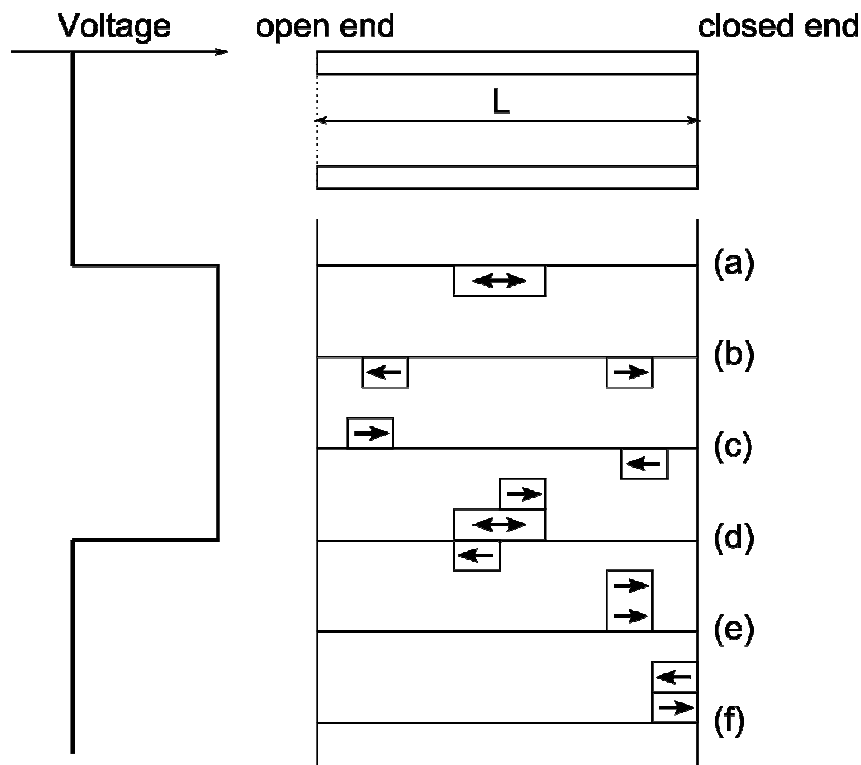


Figure 3: Wave propagation in a squeeze mode tubular piezoelectric droplet generator, adapted from [15].

In the image, a droplet generator with a cavity length L is displayed. The end of the capillary connected to the fluid reservoir can be considered as open, whereas the end with the nozzle aperture can be considered as closed, because the nozzle opening is a lot smaller than the diameter of the supply tube. When the driving signal is switched on, the actuator expands and a negative pressure is induced in the fluid chamber (a). The pressure wave splits into

two halves that propagate in opposite directions (b). The pressure waves are then reflected from the open and closed ends and propagate towards each other (c). After travelling a distance of L , the pressure waves meet in the middle and would cancel each other out. If in this moment the voltage falls down to zero, a new, positive pressure wave is created that recombines with the positive part of the initial pressure wave, while the negative part is annihilated (d). The enhanced positive pressure wave travels to the nozzle end of the capillary (e). Then a droplet is ejected and the pressure wave is reflected again (f) [15].

2.2 FORMULATION REQUIREMENTS

The task to find reliably ejectable fluids for the inkjet printing of pharmaceutical substances proved to be more challenging than anticipated. The liquids that are selected as carrier fluids for the test substances have to meet pharmaceutical as well as process technological needs. The carrier solvents should be fast drying, nonhazardous for patient and droplet generator, and preferably already approved for pharmaceutical use. Water is a preferred solvent for pharmaceutical applications, because it is able to dissolve a wide range of substances and is nontoxic. Organic solvents exhibit more favorable evaporation characteristics than water, but only few are suitable for pharmaceutical applications. The list of approved cosolvents for liquid preparations includes, for example, ethanol, isopropanol, propylene glycol, glycerol and PEG 400 [16]. In addition, the pharmaceutical droplet ejector fluids should be chemically and biologically stable over time and exhibit preferably a neutral pH.

Further requirements are a high solubility for organic compounds. The paper substrates are stripes (1.2 x 15 cm) with a low liquid absorption capacity. Therefore, it is necessary to achieve the highest possible concentration of active ingredient in a printing solution.

Viscosity, surface tension and density should be suited for DOD drop formation. According to various publications in the field of inkjet printing technology, the properties of the printed liquid have to be within certain limits [14][17].

Unfortunately, ideal drop formation conditions depend not only on the fluid properties, but also on the type and the design of the applied DOD droplet generator. In order to avoid clogging of the nozzle aperture, the pharmaceutical liquids should, if possible, not contain particles larger than one tenth of the nozzle diameter.

2.3 PHARMACEUTICAL INGREDIENTS STUDIED

Pyridoxine (B6), folic acid (FA) and cyanocobalamin (B12) were selected as model solutes for this study. Table 1 lists chemical data of the selected substances. The three molecules have significantly different molecular sizes and solubilities in water. B6 was primarily chosen for its good solubility in water. B12 is used in very low doses in pharmaceutical preparations. It is thus an appropriate candidate for precise liquid dosing. FA is almost insoluble in water and therefore suited for the preparation of aqueous suspensions. As opposed to many low dosage active pharmaceutical ingredients, the applied substances are nontoxic and show low risk potential for the experimenter.

| Name | Molecular formula | CAS-Nr. | M_r | m_p [°C] | L (H ₂ O, 25°C) [mg/ml] |
|------|---|-----------|---------|------------|------------------------------------|
| B6 | C ₈ H ₁₂ NO ₃ Cl | [58-56-0] | 205.64 | 206–212 | 220 [18] |
| FA | C ₁₉ H ₁₉ N ₇ O ₆ | [59-30-3] | 441.40 | 250 | 0.561 [19] |
| B12 | C ₆₃ H ₈₈ CoN ₁₄ O ₁₄ P | [68-19-9] | 1355.38 | 210 | 14.1 [18] |

Table 1: Chemical data of the used vitamins. M_r refer to relative molecular mass, m_p to melting point and L to the solubility of the substance in water at room temperature. Solubility of FA measured at pH 6.03.

The following sections provide some basic information concerning solubility and stability of the vitamins, which could be helpful for the preparation of liquid formulations.

2.3.1 VITAMIN B6 (PYRIDOXINE HYDROCHLORIDE)

Pyridoxine is one of six derivatives of vitamin B6 that can be chemically converted into one another. The other forms of B6 are pyridoxine-5-phosphate, pyridoxal, pyridoxamine and their corresponding 5-phosphates. Pyridoxine is a pyridine base that forms a salt with hydrochloric acid, called pyridoxine hydrochloride (figure 4). The colorless crystals are well soluble in water, ethanol and propylene glycol, and poorly soluble in methanol and acetone. Pyridoxine hydrochloride is practically insoluble in ether and chloroform [20].

Pyridoxine is less sensitive to light exposure, temperature and pH than the other vitamins [21]. Solutions kept in the dark show no significant loss of substance, not even when stored at elevated temperatures. In neutral and alkaline solutions pyridoxine degrades faster when exposed to artificial light than to natural light [22].

Vitamin B6 occurs naturally in grains, potatoes, green vegetables and legumes. The recommended daily intake is 2.0 mg for men and 1.6 mg for women [18].

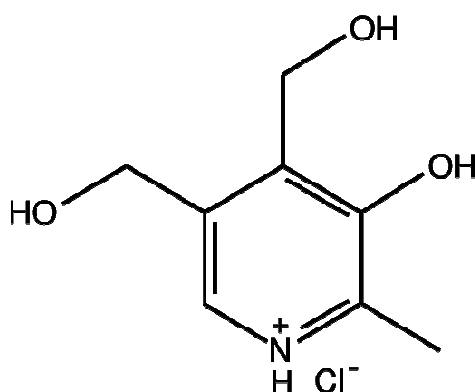


Figure 4: Chemical structure of pyridoxine hydrochloride.

2.3.2 VITAMIN B9 (FOLIC ACID)

The molecular structure of folic acid is composed of 6-methylpterin, *p*-aminobenzoid acid and L-glutamic acid (figure 5). The yellow – orange crystals are insoluble in acetone, chloroform, benzene, ether and cold water, and poorly soluble in ethanol, butanol and hot water. FA shows good solubility in pyridine, phenol, glacial acetic acid and alkaline or carbonate solution [20]. FA can be produced biotechnologically, but it is usually produced by chemical synthesis on industrial scale.

Under influence of light, vitamin B2 and oxygen, FA undergoes rapid oxidative cleavage to *p*-aminobenzoylglutamic acid and 2-amino-4-hydroxy-6-pteridinecarboxaldehyde. The reaction is pH dependent [23][24], and the exclusion of air does not stop the reaction [24]. Solutions can be stabilized by adding antioxidants [25]. Biamonte et al. found that other vitamins, like B6 and thiamine, can also have a decomposing effect on FA in solution [23]. Akhtar et al. discovered that the decomposing effect of B2 on FA is pH dependent [26] and that the photolysis of FA is faster in acidic solution than in alkaline media [27].

Folates are present in all food products, especially green leaved vegetables, liver and beans, but also in eggs. The recommended daily intake is 200 µg for men and 180 µg for women. To sustain normal folate levels during pregnancy, the required intake is significantly higher (400 µg/d). Folate deficiencies can cause macrocytic anemia and neural tube effects in developing embryos [18].

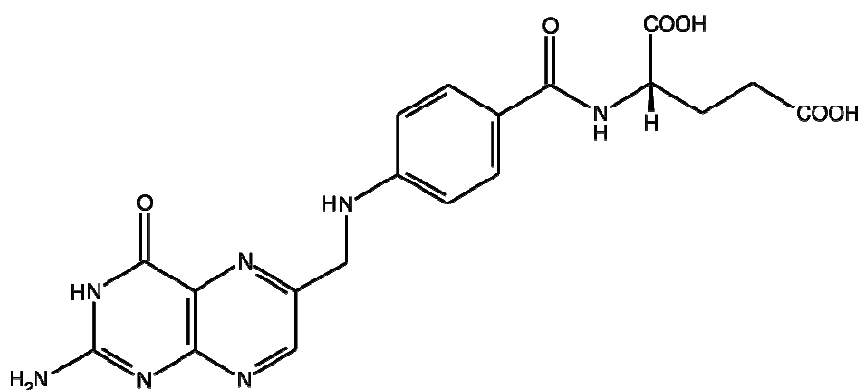


Figure 5: Chemical structure of folic acid.

2.3.3 VITAMIN B12 (CYANOCOBALAMIN)

Cyanocobalamin is a chemical complex based on a tetrapyrrole ring system with a Co atom at the center. As the name indicates, one of the six ligands is a cyanide moiety. It can only be synthesized by microorganisms and is produced exclusively via fermentation. The dark red, odorless crystals are poorly soluble in water, lower alcohols and phenols, and are insoluble in acetone, chloroform, ether and most other organic solvents. Aqueous solutions are stable at temperatures below 120°C at a pH range between 3 and 8 [18].

B12 is susceptible to photodegradation. Its primary degradation product in acidic solution, hydroxocobalmin (B12b), is less stable than B12 and can be reconverted to B12 in the presence of potassium cyanide [28]. DeMerre et. al. found that exposure to artificial light induces a higher degradation rate than to natural light and UV light [29].

Ahmad et al. analyzed the pH dependency of the photolysis reaction. The degradation is a zero order reaction that is fastest at pH 1. In general, pH values < 6 favor the light - induced reaction of B12 to B12b, above pH > 9 the amide groups are hydrolyzed [30].

B12 is ingested with animal products, and the daily requirement of B12 for humans is 5 µg [18]. B12 deficiency can therefore be caused by either eschewal of animal products in a diet or malabsorption of B12, resulting in pernicious anemia [18].

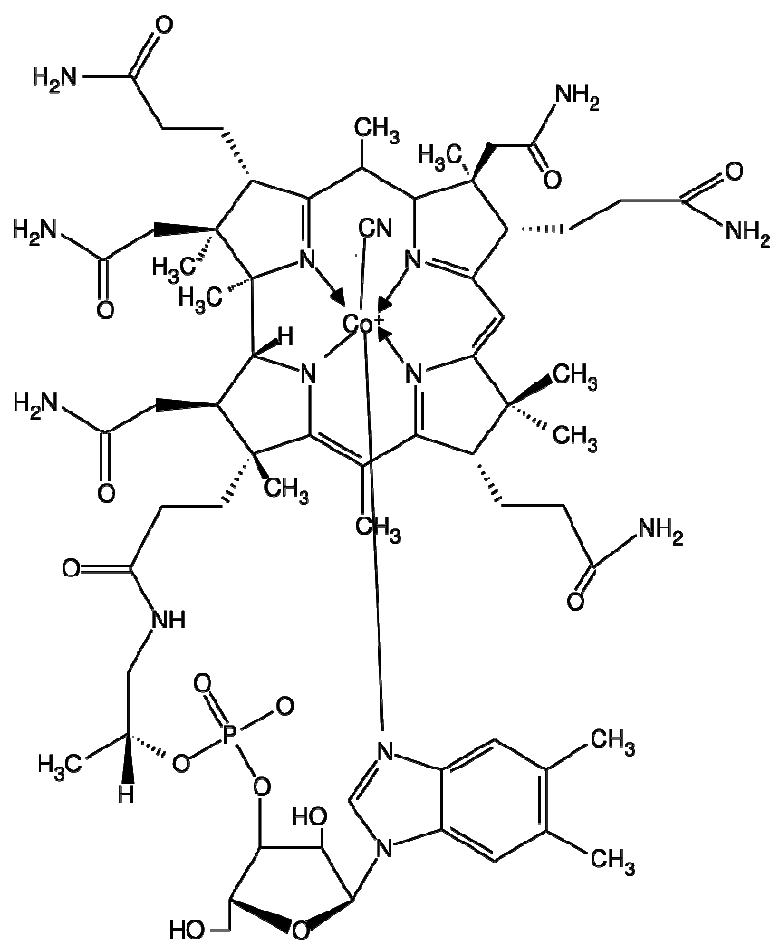


Figure 6: Chemical structure of cyanocobalamin.

2.4 COATINGS

Pharmaceutical products are often sensitive to environmental conditions like temperature, humidity, light and oxygen. Solid dosage forms, like tablets, are therefore usually coated with protective films that create barrier layers. Tablet coating can also improve process conditions by protecting filling machines from dust particles or reducing friction. Protective polymer coatings not only protect the pharmaceutical substances from degradation, but also factory staff from exposure to potentially hazardous medication dusts. Tablet coating is also important for controlled-release applications. Through application of polymers with pH dependent solubility it is possible to target specific parts of the digestive tract, thus improving the effectiveness of medications. Another purpose for film coating is the masking of unpleasant odors or flavors.

Formulations for tablet coatings are usually not only composed of polymer and solvent. They also contain excipients like plasticizers that modify the physical and mechanical properties of the film building material [31].

For this study, two protective coatings were selected for the application as a barrier layer on paper substrates. The aim was to deposit coating material on top of printed pharmaceutical substances using an inkjet printhead. The used polymers are described in the following.

Eudragit L 100-55 (CAS-Nr. [252212-88-8]) is an anionic copolymer with methacrylic acid and ethylacetate moieties in a 1:1 ratio. Figure 7 shows a monomer unit of Eudragit L 100-55. The polymer is commercially available as white powder which can be redispersed in water. It is soluble in methanol, ethanol, isopropyl alcohol, acetone and in 1 N sodium hydroxide. It is insoluble in ethyl acetate, dichloromethane, petroleum ether and water. The average relative molecular weight of Eudragit L 100-55 is approximately 250000. According to the manufacturer's data sheet, the particle size is less than 0.25 μm for 95% of all particles. Eudragit L 100-55 is insoluble at a pH lower than 5.5. Therefore it is used as an enteric coating intended to protect a solid dosage form from gastric fluids.

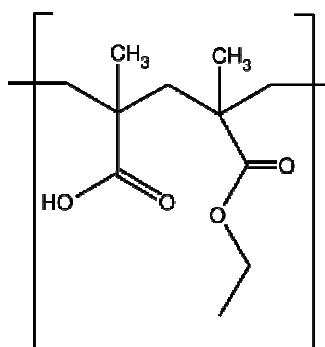


Figure 7: Monomer unit of Eudragit L 100-55 polymer.

Eudragit E 100 (CAS-Nr. [24938-16-7]) is a cationic polymer based on dimethylaminoethyl and neutral methacrylic esters. The monomer unit of Eudragit E 100 is displayed in figure 8. The slightly yellow granules have a characteristic amino-like odour. It is soluble in methanol, ethanol, isopropyl alcohol, ethyl acetate, dichloromethane and 1 N hydrochloric acid. The average relative molecular weight of Eudragit E 100 is approximately 150000. For at least 90% of all particles, the particle size is less than 0.315 μm .

E 100 is used as a plain insulating coating that protects solid dosage forms like tablets from humidity and air. It is soluble in gastric fluids below pH 5, but not in saliva.

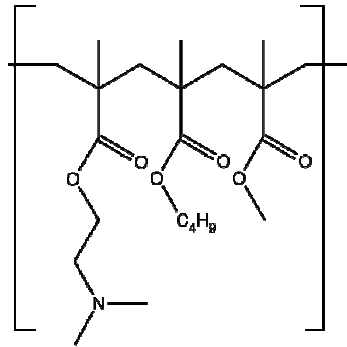


Figure 8: Monomer unit of Eudragit E 100 polymer.

3 MATERIALS AND METHODS

3.1 MATERIALS

3.1.1 CHEMICALS

Ethanol denaturated (EtOH denat.) 99.8% wt + 1% wt MEK, isopropyl alcohol (iPrOH) 99.9% wt, acetone 99.5% wt, propane-1,2-diol (PG) 99.5% wt and glycerol 98% wt were purchased from Carl Roth (Karlsruhe, Germany). Ethanol LiChroSolv (EtOH) 99.9% wt was purchased from MERCK (Darmstadt, Germany). Pyridoxine hydrochloride (vitamin B6), cyanocobalamin (vitamin B12) and folic acid (FA) were obtained from G.L. Pharma (Lannach, Austria) and were of pharmaceutical grade. Polyethylene glycol (PEG) and polysorbate 20 (T20) were purchased from Clariant (Muttenz, Switzerland) and Cognis (Monheim, Germany), respectively. Acetic acid >99% wt was purchased from Sigma - Aldrich (Vienna, Austria) and acetonitrile LC-MS grade was obtained from Bartelt (Graz, Austria). Eudragit L 100-55 and Eudragit E 100 were kindly provided by Evonik Industries. Cigarette plug wrap paper was kindly provided by the Delfort paper group.

3.1.2 SOLVENTS AND SOLVENT MIXTURES

Several solvents and solvent mixtures (see table 2) which were suitable for pharmaceutical preparations and DOD drop formation were included in the study of drop formation. All liquids were suitable for oral application in small amounts [32][16].

| Composition | Reference |
|-------------------------------------|------------------|
| H ₂ O/EtOH:7/3 | - |
| PG/H ₂ O:3/1 | [14] |
| PG/H ₂ O:1/1 | [14] |
| 48% wt glycerol in H ₂ O | [33] |

Table 2: Mixtures of solvents used in this study. Mixture compositions refer to volume ratios and percentages to mass. In addition H₂O, EtOH and iPrOH as pure solvents have also been tested.

The H₂O/EtOH mixture was included because vitamin B12 showed good solubility in it. Mixtures of propylene glycol (PG) and H₂O were recommended by Lee as reliable liquids to test the function of a DOD droplet generator, due to their stable formation of monodisperse

drops [14]. The glycerol mixture was already successfully used in a series of DOD experiments conducted by Dong et al. [33].

3.1.3 SOLUTIONS

All solutions were freshly prepared for each experiment and were stirred at room temperature using a magnetic stirrer until a clear solution was obtained. To avoid photodegradation [29] [30], the B12 solutions were protected from light using aluminum foil. Solvent mixtures were prepared in advance. Composition and concentration of the solutions are listed in table 3 below.

| Composition | API | Concentration [mg/ml] |
|----------------------------------|----------------|------------------------------|
| B12 in H ₂ O/EtOH:7/3 | Cyanocobalamin | 40 |
| B12 in EtOH/H ₂ O:7/3 | Cyanocobalamin | 20 |
| B12 in PG/H ₂ O:3/1 | Cyanocobalamin | 40 |
| B12 in PG/EtOH:3/1 | Cyanocobalamin | 40 |
| B6 in H ₂ O | Pyridoxin-HCl | 180 |
| FA in 1 M NaOH | Folic acid | 180 |
| 5% PEG 300 in H ₂ O | - | 50 |

Table 3: Compositions and concentrations of several vitamin preparations and one polymer solution. Mixture compositions refer to volume ratios and percentages to mass.

3.1.4 SUSPENSIONS

Several suspensions with varying folic acid and surfactant content were prepared at the Institute of Pharmaceutical Technology (University of Graz) by Daniela Strohmaier.

For this purpose 10 % wt of folic acid were suspended in an aqueous 3 % wt Tween 20 solution and homogenized using a Panda 2K, NS1001L Spezial high-pressure homogenizer (GEA Niro Soavi, Lübeck, Germany). In batches of 50 ml the dispersions were homogenized, running 2 cycles at 500 bar followed by 30 cycles at 1000 bar. To prevent folic acid degradation during homogenization, the temperature was kept at 5 °C.

After preparation, the suspensions were analyzed for particle size and zeta potential and stored in a refrigerator. Before the fluid was filled into the droplet generator it was prefiltered using a 5 µm PTFE syringe filter (ReZist 30 PTFE, Whatman, Maidstone, UK).

A list of the obtained suspensions, their composition, mean particle size and zeta potential are presented in table 4.

| FA content [%] | Surfactant [%] | Particle Size [nm] | Zeta potential [mV] |
|----------------|----------------|--------------------|---------------------|
| 1 | 1 | 457.8 | -49,4 |
| 1 | 2 | 507.1 | - 42.2 |
| 1 | 3 | 333.5 | -49.6 |
| 5 | 3 | 444.6 | -48.1 |
| 10 | 3 | 373.3 | -50.7 |
| 15 | 3 | 447.9 | -54.1 |
| 20 | 3 | 348.8 | -51.5 |

Table 4: Folic acid suspensions with differing API and surfactant content. The mean particle size and zeta potential were measured shortly after preparation. Percentages refer to weight percent.

3.1.5 POLYMER COATINGS

An overview of the used polymers is given in table 5.

| Trade name | Polymer type | Commercial form | Solubility |
|-------------------|--------------|---------------------|------------|
| Eudragit L30 D-55 | anionic | dispersion (30% wt) | pH >5.5 |
| Eudragit L 100-55 | anionic | powder | pH >5.5 |
| Eudragit E 100 | cationic | granulate | pH <5 |

Table 5: Commercially available types of methacrylate copolymers used in this study.

Eudragit L 30 D-55 is a commercially available ready-to-use dispersion of 30% wt L 100-55 in water. The aqueous dispersion was used undiluted and without film building additives.

In addition, three different solutions of Eudragit were tested.

- a) 15% wt of L 100-55 in EtOH
- b) 1.5% wt of L 100-55 in EtOH
- c) 1% wt E 100 in mixture of iPrOH, acetone and H₂O

For solution a), 15 g of Eudragit L 100-55 was dissolved in 85 g of a previously prepared mixture of 97 g of denaturated EtOH and 3 g of H₂O deion at room temperature using magnetic stirring. Solution b) was diluted from solution a) with denaturated EtOH. For solution c) 1 g Eudragit E 100 was dissolved in a prepared mixture of 57.3 g of iPrOH, 38.8 g of acetone and 2.9 g H₂O de-ion at room temperature using magnetic stirring.

3.1.6 PAPER

In the drop impact behavior study, a commercially available plug wrap paper for cigarettes and laboratory papers were tested for their qualities as printing substrates.

The plug wrap paper (“H”) had a grammage of 24 g/cm² and was made from wood fiber. It also contained 13.5% CaCO₃ as a filling pigment.

Two types of laboratory papers were investigated. Both had a grammage of 40 g/cm² and were produced with bleached hardwood kraft, but contained different fillers (TiO₂ and CaCO₃). All papers, with the exception of “H”, served as printing substrates in the conducted dissolution tests.

| Paper | Fiber | Filler | Grammage [g/cm ²] | Filler content [%] |
|-------------------|-------------------------|-------------------|-------------------------------|--------------------|
| H | Wood | CaCO ₃ | 24 | 13.5 |
| CaCO ₃ | Bleached Hardwood Kraft | CaCO ₃ | 40 | 30 |
| TiO ₂ | Bleached Hardwood Kraft | TiO ₂ | 40 | 30 |

Table 6: Properties of papers used for drop impact studies and dissolution testing.

3.2 EXPERIMENTAL SETUP AND IMAGE PROCESSING

3.2.1 SETUP FOR DROP DIAMETER AND VELOCITY MEASUREMENTS

A diagram of the setup used for the characterization of droplet formation, and for measuring the drop diameter and velocity, is shown in figure 9. It consists of a commercially available DOD-droplet generator (type MD-K-140) by Microdrop Technologies (Norderstedt, Germany) with an inner nozzle diameter of 100 μm and a liquid reservoir with a volume of 4 ml. It is mounted on a home-made movable xyz-stage, which can be positioned within micrometer precision.

The droplet generator is controlled with a control unit (type MD-E-201-H), which provides the excitation signal for the piezo actuator and the interface to the computer. The enclosed control software allows the variation of the following operating parameters: The pulse width of the excitation signal can be varied between 5 and 255 μs, the pulse amplitude between 30 and 255 V, the pulse frequency between 1 Hz and 6 kHz. It also contains a pressure unit which creates negative internal pressures up to 50 mbar in the capillary to avoid leaking of the operating fluid an ensuring a reliable drop formation [14]. A separate heating unit can be

used to heat up the nozzle and the liquid reservoir of the device to temperatures in the range of 25°C to 80°C and 25°C to 100°C, respectively.

The droplet visualization is based on backlight illumination with a strobed light source (red LED), which is synchronized with the driving signal of the droplet generator. The delay of the signal driving the LED against the actuator signal producing the drops can be varied in the range of 0 to 2 ms. A Toshiba Teli monochrome CCD camera (type MD-O-539-20) with a 10x magnification and a framing rate of 50 Hz was used to record droplet images.

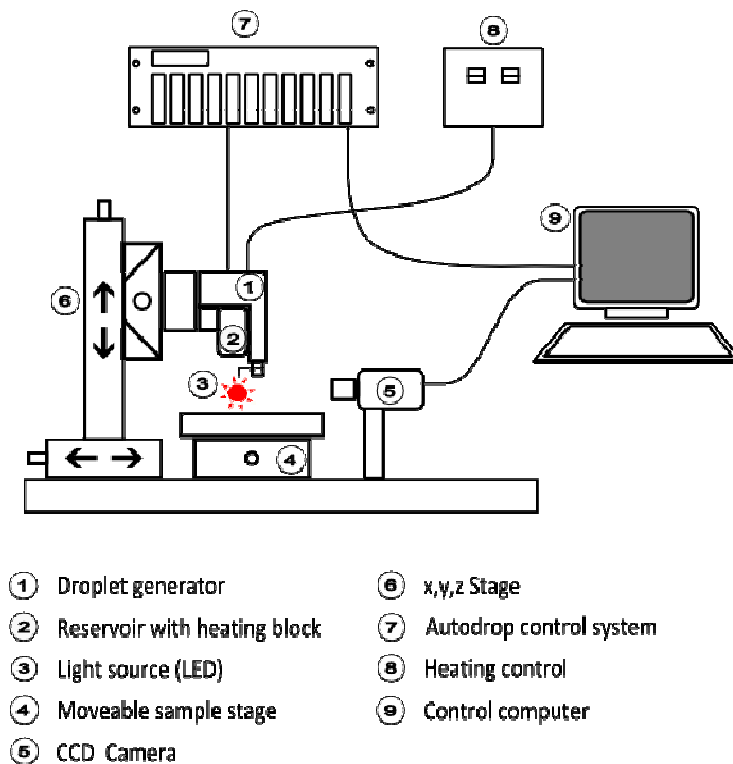


Figure 9: Schematic setup for drop formation and drop diameter and velocity measurements.

3.2.2 SETUP FOR DROPLET MASS MEASUREMENTS

The setup used for droplet gravimetry is shown in figure 10. A Sartorius microbalance (type ME36S) with housing and a readability of 0.1 μg (repeatability of $\pm 2 \mu\text{g}$) placed on a weighting table was used. The droplet generator was removed from the sample stage, mounted on a laboratory stand and positioned as close as possible to the weighting vessel. To minimize the liquid evaporation and air drafts, the nozzle was enclosed with an extra covering. The control unit was placed on a separate table nearby. A Sartorius balance printer (type YDPO3-OCE) was set to record balance readings automatically in 10 s intervals.



Figure 10: Setup used for droplet mass measurements.

3.2.3 SETUP FOR IMPACT BEHAVIOR TESTS

The apparatus for the drop impact tests was basically the same as described in section 3.2.1, with the exception of the camera and the light source. Instead of the CCD camera, high-speed camera by Integrated Design Tools, Inc. (type M3) with a maximum frame rate of 31000 fps at 1280 x 16 pixels and a 12 x objective were applied. A Storz “techno light 270” endoscope served as the light source providing a bright uniform background illumination.

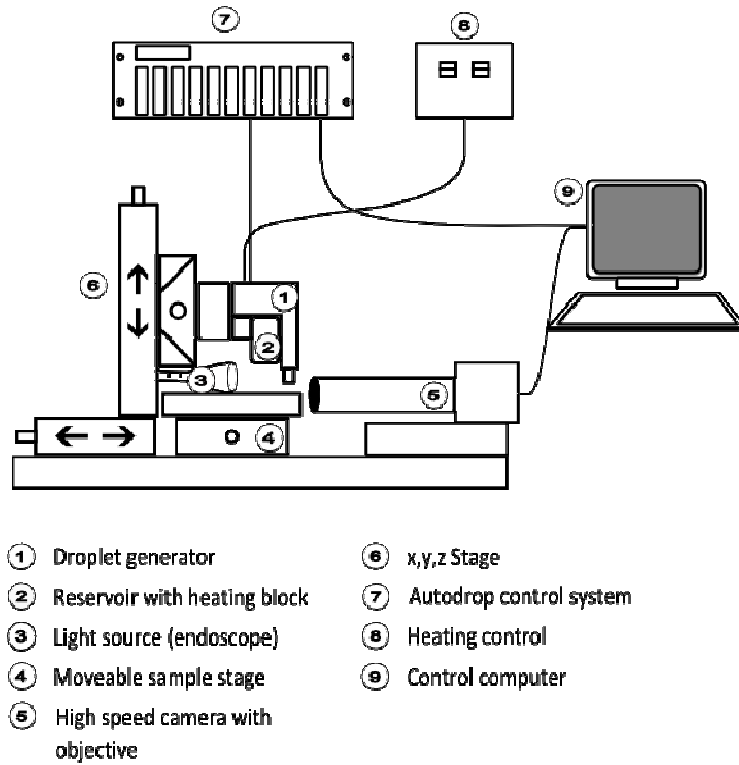


Figure 11: Schematic setup for impact behavior tests.

3.3 METHODS

3.3.1 PHYSICAL CHARACTERIZATION OF THE LIQUIDS

To produce uniformly sized, single droplets, the physical characteristics of the ejected liquid must be within certain limits. The liquid properties considered relevant for DOD drop formation are density, shear viscosity and surface tension against air [14]. To gain information concerning the wettability of the glass capillary, especially at the nozzle aperture, the contact angle at the three-phase contact line between glass, liquid and air was measured as well.

3.3.1.1 DENSITY MEASUREMENT

The liquid density and sound speed were measured using the oscillating tube device DSA 5000M by Anton Paar. 3 ml of sample volume were injected into the U-tube, carefully avoiding the creation of air bubbles using a disposable syringe. 3 measurements per sample were carried out at a temperature of 20.00°C, and the results were averaged. After each measurement the U-tube was rinsed thoroughly with at least 10 ml of de-ionized water and

with 5 ml of ethanol (99.9% wt). The U-tube was allowed to dry completely before injecting a new sample.

3.3.1.2 SURFACE TENSION MEASUREMENT

The surface tension measurements were carried out on a contact angle measurement device by Krüss (FM40Mk2 Easy Drop) using the pendant drop method. A drop was released from a capillary with a diameter of 1.825 mm until a pendant drop was formed. The drop shape is determined using a camera and special fitting software. Knowing the contour of the droplet and the density of the liquid, the surface tension is calculated automatically by the software. The surface tension was measured for a time period of 5 to 10 seconds, and the values were averaged. For every liquid at least 10 droplets were measured.

Between two different liquids, the capillary was rinsed carefully with de-ionized water, and the tip was wiped with a special cleaning wipe. All surface tension measurements were carried out at room temperature between 25 and 28°C.

3.3.1.3 DYNAMIC VISCOSITY MEASUREMENTS

The dynamic viscosity was measured with a shear rheometer by Anton Paar (MCR300) in a double-gap cylinder system, which is ideally suited for low viscosity liquids.

In every run, 4 to 4.5 ml of sample were analyzed, and 11 measuring points were recorded. Every measurement was performed 3 times, and the results for each series were averaged. After three measurements, a new liquid sample was injected.

The shear rate was varied between 1 and 100 s⁻¹ at a constant temperature of 20°C. In addition, the temperature was varied at constant shear rates of 100 s⁻¹ and 500 s⁻¹.

3.3.1.4 CONTACT ANGLE MEASUREMENTS

The contact angle was measured against a pre-cleaned glass plate using a Krüss contact angle measurement device (FM40Mk2 Easy Drop). The glass was cleaned in isopropyl alcohol (99.9% wt) in an ultrasonic bath for 10 minutes at room temperature. After that, the glass was rinsed with de-ionized water and with ethanol (99.9% wt) and allowed to dry for at least 1 week in a laboratory oven at 80°C. The glass plates were kept in a clean glass jar until the measurement.

A droplet of 5 μl volume was placed on the cleaned glass plate. Using the computer software of the instrument, the contour of the droplet was determined, and the angle between the glass surface and the liquid phase was calculated using the circle fitting method, which is recommended for small contact angles $< 30^\circ$. The contact angle was measured for a time period of 10 seconds, and these results were averaged. At least 10 droplets per liquid were measured.

3.3.2 DIMENSIONAL ANALYSIS

The applied method was based on a matrix transformation described in detail by Zlokarnik [34]. The first step is to determine the relevance list which consists of all physical variables influencing the DOD drop formation. From these parameters, a dimensional matrix is constructed which then is divided into a core matrix B and a residual matrix R. Using Matlab, the inverse matrix of B was calculated followed by multiplication of the inverse of B with the residual matrix R. From the resulting matrix, 5 dimensionless numbers were formed. Where necessary, the dimensionless numbers were transformed into more suitable or common dimensionless numbers. Since the results are dependent on which parameters are put into the core and which into the residual matrix, this procedure was carried out for every possible combination of variables. The obtained dimensionless numbers were then combined to a product of powers of the form

$$\Pi_t = A \cdot \Pi_1^{a_1} \cdot \Pi_2^{a_2} \cdot \Pi_3^{a_3} \cdot \Pi_4^{a_4} \quad (1)$$

where Π_t is the target quantity and A is a constant.

3.3.3 DROPLET GRAVIMETRY

The experiment is based on the work by Verkouteren and Verkouteren, who developed a gravimetric method to measure the mass of droplets ejected by a drop-on-demand droplet generator [35]. This experiment was carried out using the setup presented in section 3.2.2.

Two liquids showing very different physical characteristics, H_2O and vitamin B12 in PG/ H_2O :3/1, were used in this experiment.

A Sartorius balance printer (model YDPO3-OCE) was set to record time-stamped balance readings in 10 second intervals. The droplet generator was positioned as close as possible to

the weighting vessel to ensure that the droplets were ejected into it. The evaporation rate was observed by placing liquid in the weighting vessel (usually the same liquid which is ejected, but for the B12 propylene glycol/water mixture, paraffin oil was used, because propylene glycol is hygroscopic, see figure 12). Two different ejecting modes were applied. Setting the droplet generator to burst mode allows the dispensing of a fixed number of droplets. Between two bursts the evaporation rate was observed for at least two minutes. 10 single bursts which consisted of 100, 1000 or 10000 droplets were ejected in each measurement. In the continuous mode a droplet jet is ejected continuously for two minutes. Before and after the measurement of mass increase the evaporation rate is observed for 2 minutes. A summary of the experimental conditions is given in table 7.

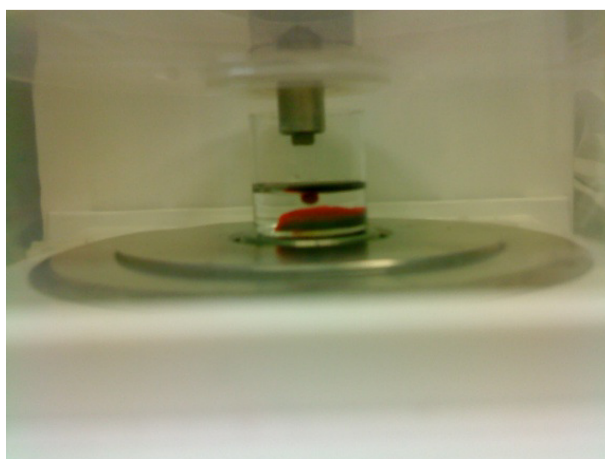


Figure 12: Drop ejection of a B12 solution (red) into paraffin oil.

| Gravimetric methods | | | |
|----------------------------|--------------------------------|---|--|
| Method | Liquid | Ejected amount | Operating parameters |
| Burst | H ₂ O dd | 100 and 1000 droplets 10000 droplets | 100 V, 25 μs, 100 Hz 100 V, 25 μs, 200 Hz |
| | B12 in PG/H ₂ O:3/1 | 100, 1000 and 10000 droplets | 115 V, 30 μs, 1000 Hz |
| Continuous | H ₂ O dd | Continuous ejection for 2 minutes, then 2 min no ejection | 100 V, 25 μs, 200 Hz |
| | B12 in PG/H ₂ O:3/1 | Continuous ejection for 2 minutes, then 2 min no ejection | 115 V, 30 μs, 1000 Hz |

Table 7: Operating parameters of the gravimetric methods applied.

3.3.4 DISSOLUTION TESTING

To investigate the release properties of the paper carrier, on which droplets were deposited, dissolution tests of several substances were performed using an Erweka DT 820 device.

Paper substrates were imprinted with test substances (B12, Na-folate and suspended folic acid) and were then stored in the dark at room temperature until analysis. Table 8 provides an overview on the experimental conditions.

To simulate gastric fluids, the dissolution tests were carried out in 0.1 M HCl at 37°C. Applying the paddle apparatus method, 3 to 6 samples were stirred continuously at 100 rpm in 500 ml liquid volume per dissolution vessel. Every 5 minutes for the duration of 45 minutes, 1 ml samples were drawn from each vessel. The disintegrated fiber content was separated by centrifugation at 9500 rcf (g) for 10 minutes. 500 µl of supernatant were subsequently analyzed using a reverse phase HPLC-UV/MS method modified after Heudi et al [36] to quantify the printed substances.

Measurements were performed using an ACQUITY UPLC H-Class Bio system (Waters, Milford, U.S.A) with a Sample Manager-FTN autosampler, a quaternary solvent manager and a PDA detector. A reverse-phase ACQUITY UPLC BEH C18 1.0 x 50 mm (1.7 µm particle size) column (Waters, Milford, U.S.A) was used to separate the sample. 10 µl of sample were injected. Aqueous 0.15% wt acetic acid solution and acetonitrile were applied as the mobile phase in a gradient elution with a flow rate of 0.4 ml/min. The test substances were quantified by means of UV-spectra recorded at 275 nm.

| Substance | Formulation | DOD Operating parameters | Drop diameter | Amount |
|------------------|--|---------------------------------|----------------------|---------------|
| B12 | 40 mg/ml in PG/H ₂ O:3/1 | 1000 Hz, 115 V, 30 µs | 78.6 µm | 250 µg |
| Na-folate | 180 mg/ml FA in 1 M NaOH | 1000 Hz, 103 V, 24 µs | 68.5 µm | 5 mg |
| FA | 10% wt suspended in H ₂ O, 3% wt T20 | 1000 Hz, 90 V, 26 µs | 74 µm | 5 mg |

Table 8: Operating parameters and preparations used in dissolution testing.

4 PHYSICAL PROCESSES INVESTIGATED

4.1 DROPLET FORMATION PROCESS

The droplet formation process was observed using the experimental setup described in section 3.2.1. Varying the delay between the signals to the droplet generator and to the illuminating LED, different stages in the development of a drop were visualized at fixed operation parameters. Pictures were taken at low drop formation frequencies (usually 100 or 200 Hz) and signal voltages and pulse widths, which ensured a stable and disturbance free drop formation. The strobe delay was varied in steps of 20 μs from 10 to 300 μs and in 100 μs steps from 300 to 1000 μs . The pinch off of the droplet from the liquid filament was also marked. Differences in the dilatation and pinch off behavior were observed.

4.2 DROPLET DIAMETER AND VELOCITY

For the present studies, the experimental setup in section 3.2.1 was used. Stroboscopically illuminated images of droplets were recorded at many different operation settings. The images were analyzed using a home-made Matlab routine and in some cases the freeware ImageJ . After defining a region of interest, the image is converted into a black and white image, showing a black droplet against a white background. This image is then converted into its negative, showing a white droplet against a black background. The software extracts the contour line of the droplet and calculates the diameter, surface and volume of the droplet (figure 13a).

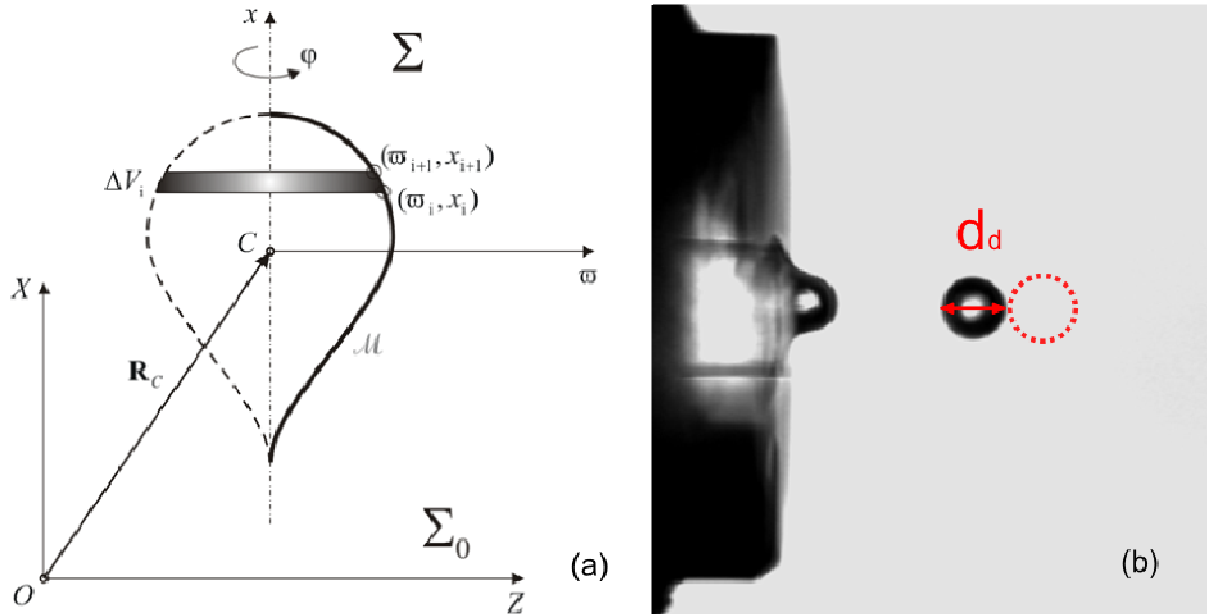


Figure 13: (a) Principle of surface and volume determination for axially symmetric bodies [37]. (b) Illustration of droplet velocity determination.

To measure the velocity of the droplet, two images at the same operating settings but different stroboscopic delay were recorded. The droplet velocity is calculated from an image, which is taken right after the droplet's pinch off from the liquid filament, taking a spherical shape for the first time, and an image taken as the drop appears one diameter downstream (see figure 13b).

4.3 DROP IMPACT

If a drop impacts on a solid, dry substrate, in most cases one of two outcomes can occur. Usually a drop is either deposited or splashed when it impacts on a substrate, depending on its impact velocity and the properties of fluid and substrate. The result of a drop impact is directly influenced by a series of factors, i.e. drop size, impact velocity and direction relative to the surface normal [38][39], viscosity, density, viscoelasticity, surface and interfacial tension as well as roughness and wettability of the surface [38]. Figure 14 illustrates the two main outcomes droplet deposition and splashing with corona formation.

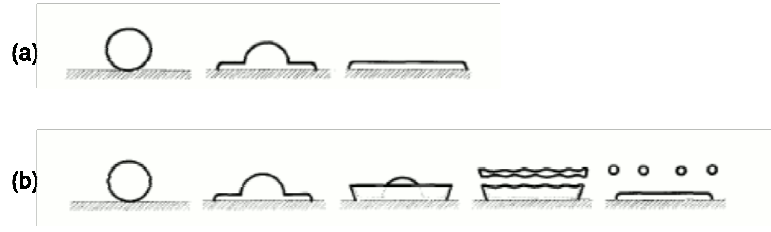


Figure 14: Schematic image of drop impact. (a) Deposition with liquid film formation and (b) splashing with disintegration into secondary droplets (b) [38].

The necessary condition for splashing upon impact is that the kinetic energy of the drop exceeds the surface energy required to form new droplets [14][38][40]. Much like drop formation, impact can also be described in terms of dimensionless numbers. The most important dimensionless terms are the Ohnesorge number Oh , the Weber number We and the Reynolds number Re . The numbers are inter-related as per $Oh = (We)^{0.5}/Re$.

$$Oh = \frac{\mu}{\sqrt{d_d \sigma \rho}} \quad (2)$$

$$Re = \frac{\rho d_d u}{\mu} \quad (3)$$

$$We = \frac{\rho d_d u^2}{\sigma} \quad (4)$$

Depending on the Froude number, gravitational forces are also involved in drop impact reactions. For micro drops smaller than 100 μm in diameter, however, drop impact is primarily governed by surface energy effects [14].

The present case focuses on the investigation of the impaction of micro droplets in direction normal to the surface of a dry absorbing substrate with an uneven surface structure.

For the drop impact study, the setup described in section 3.2.3 was used. Tests were conducted on glass (reference), hand-made paper with TiO_2 or CaCO_3 filling, commercially available cigarette paper (“H”) and standard reprographic paper (“Copy”). These substrates vary in roughness, absorption capacity and porosity. To maximize the frame rate, the smallest possible image size to capture the drop impact was used. That way, a frame rate of 8000 fps was achieved, setting two captures 125 μs apart. The droplet generator was set to continuous mode with a drop frequency of 30 Hz, because single burst droplets often showed satellites and droplets produced at lower frequencies were not placed accurately enough on the substrate to be observed. In order to avoid multiple droplets impinging on the same spot, the droplet generator was moved with maximum speed past the camera. The liquids used in these tests were de-ionized water, vitamin B12 dissolved in PG/ H_2O :3/1, folic

4 Physical Processes Investigated

acid dissolved in 1 M NaOH and a 10% wt folic acid suspension in H₂O dd. A summary of the applied operation parameters is presented in table 9.

Each impact test was repeated at least five times.

| Liquid | H ₂ O deion. | B12 PG/H ₂ O:3/1 | FA in NaOH | FA sus (10% wt) |
|----------------------------|-------------------------|-----------------------------|------------|-----------------|
| Frequency [Hz] | 30 | 100 | 30 | 30 |
| Pulse amplitude [V] | 100 | 120 | 110 | 100 |
| Pulse width [μs] | 25 | 25 | 25 | 27 |
| Mode | C | B | C | C |

Table 9: Operating parameters used in the droplet impact study. Letters C and B refer to continuous and burst mode, respectively.

5 RESULTS AND DISCUSSION

5.1 LIQUID PROPERTIES

This section presents the results of density, surface tension, dynamic viscosity and contact angle measurements. In addition rheological tests and the corresponding flow curves for the inkjet test liquids are shown. Table 10 displays the measured fluid properties of the investigated test liquids.

| Liquid | Density [kg/m ³] | STD | Surface tension [mN/m] | STD | Dyn. Visc. [mPas] | STD |
|-----------------------------------|---------------------------------|----------|---------------------------|------|----------------------|----------|
| H ₂ O | 998.25 | 1.15E-02 | 72.02 | 0.20 | 1.01 | 3.17E-02 |
| EtOH | 790.25 | 1.10E-01 | 21.42 | 0.35 | 1.19 | 1.42E-02 |
| iPrOH | 785.33 | 2.21E-01 | 20.58 | 0.20 | 2.35 | 2.70E-02 |
| H ₂ O/EtOH:7/3 | 963.16 | 1.55E+00 | 37.13 | 0.46 | 2.62 | 6.50E-02 |
| PG/H ₂ O:3/1 | 1043.68 | 2.02E-01 | 33.22 | 0.11 | 21.40 | 1.83E-02 |
| PG/H ₂ O:1/1 | 1038.88 | 1.07E+00 | 44.21 | 0.11 | 7.68 | 1.06E-02 |
| 48% wt gly in H ₂ O | 1120.47 | 4.64E-02 | 69.57 | 0.39 | 5.29 | 1.65E-02 |
| B12 in H ₂ O/EtOH:7/3 | 975.00 | 1.96E+00 | 35.93 | 0.61 | 2.00 | 7.44E-02 |
| B12 in EtOH/H ₂ O:7/3 | 885.60 | 2.55E-01 | 26.06 | 0.19 | 2.21 | 8.34E-03 |
| B12 in PG/H ₂ O:3/1 | 1051.97 | 2.84E+00 | 38.96 | 0.05 | 21.00 | 1.83E-02 |
| B12 in PG/EtOH:3/1 | 986.89 | 2.38E-01 | 30.90 | 0.39 | 29.43 | 9.52E-02 |
| B6 in H ₂ O | 1045.80 | 2.69E-01 | 68.90 | 0.94 | 1.79 | 2.40E-01 |
| FA in 1 M NaOH | 1073.46 | 3.69E-01 | 69.54 | 0.71 | 4.32 | 4.51E-02 |
| 5% wt PEG 300 in H ₂ O | 1006.08 | 3.57E-01 | 64.28 | 0.12 | 1.30 | 2.49E-02 |
| FA-Sus (1% wt, 2% wt T20) | 1001.40 | 1.68E+00 | 33.84 | 0.46 | 1.23 | 1.17E-02 |
| FA-Sus (1% wt, 3% wt T20) | 1005.47 | 7.02E-02 | 29.90 | 0.44 | 1.29 | 3.27E-02 |
| FA-Sus (5% wt, 3% wt T20) | 1019.44 | 1.08E-01 | 31.50 | 0.40 | 1.54 | 1.01E-01 |
| FA-Sus (10% wt, 3% wt T20) | 1033.22 | 6.95E-02 | 39.31 | 0.25 | 1.61 | 4.22E-02 |
| FA-Sus (15% wt, 3% wt T20) | 1066.37 | 3.46E-01 | 36.58 | 0.21 | 1.88 | 7.02E-02 |
| FA-Sus (20% wt, 3% wt T20) | 1078.83 | 1.12E+00 | 34.73 | 0.39 | 2.57 | 1.31E-01 |

Table 10: Physical properties of the investigated test liquids at 20°C. STD is the standard deviation of the measured values. Dynamic viscosity values were measured at a shear rate of 100 s⁻¹.

The liquid density ranged between 785 (2-propanol) and 1120 kg/m³ (48% wt glycerin in H₂O), the surface tension varied between 20 (2-propanol) and 72 (water) mN/m and the dynamic viscosity between 1 (water) and 30 mPas (vitamin B12 in propylene glycol/ethanol:3/1). Furthermore the test liquids were investigated more closely concerning their rheological properties. Measurements of dynamic viscosity at a constant shear rate, varying the temperature between 20°C and 30°C, were carried out to determine the liquids fluid behavior. These measurements are discussed in the following section.

5.1.1 RHEOLOGICAL PROPERTIES

In order to gain information about the ejectability of the produced pharmaceutical liquids, a series of rheological experiments were conducted. Rotational experiments were performed in a double gap cylinder system according to the procedure given in section 3.3.1.3. The dynamic viscosity was measured as a function of shear rate to determine if any of the liquids exhibited non-newtonian flow behavior. Thus the shear rate was varied within a range of 1 - 100 s⁻¹ at a constant temperature of 20°C.

Since the DOD print head allowed for temperature adjustment to decrease ink viscosity, the temperature/viscosity relation was also investigated. Therefore, the dynamic viscosity was determined as a function of temperature at fixed shear rates of 100 and 500 s⁻¹. Data points were collected for a temperature range of 20 – 30 °C. The process temperature was kept within this temperature range to minimize the risk of vitamin degradation due to thermal influences.

As seen in figure 15 the dynamic viscosity decreases linearly with increasing temperature. This behavior is typical and well known for most liquids. The highest viscosity was found for B12 in PG/EtOH:3/1. Also, the dynamic viscosity decreases more rapidly for the PG mixture than for the other mixtures.

5 Results and Discussion

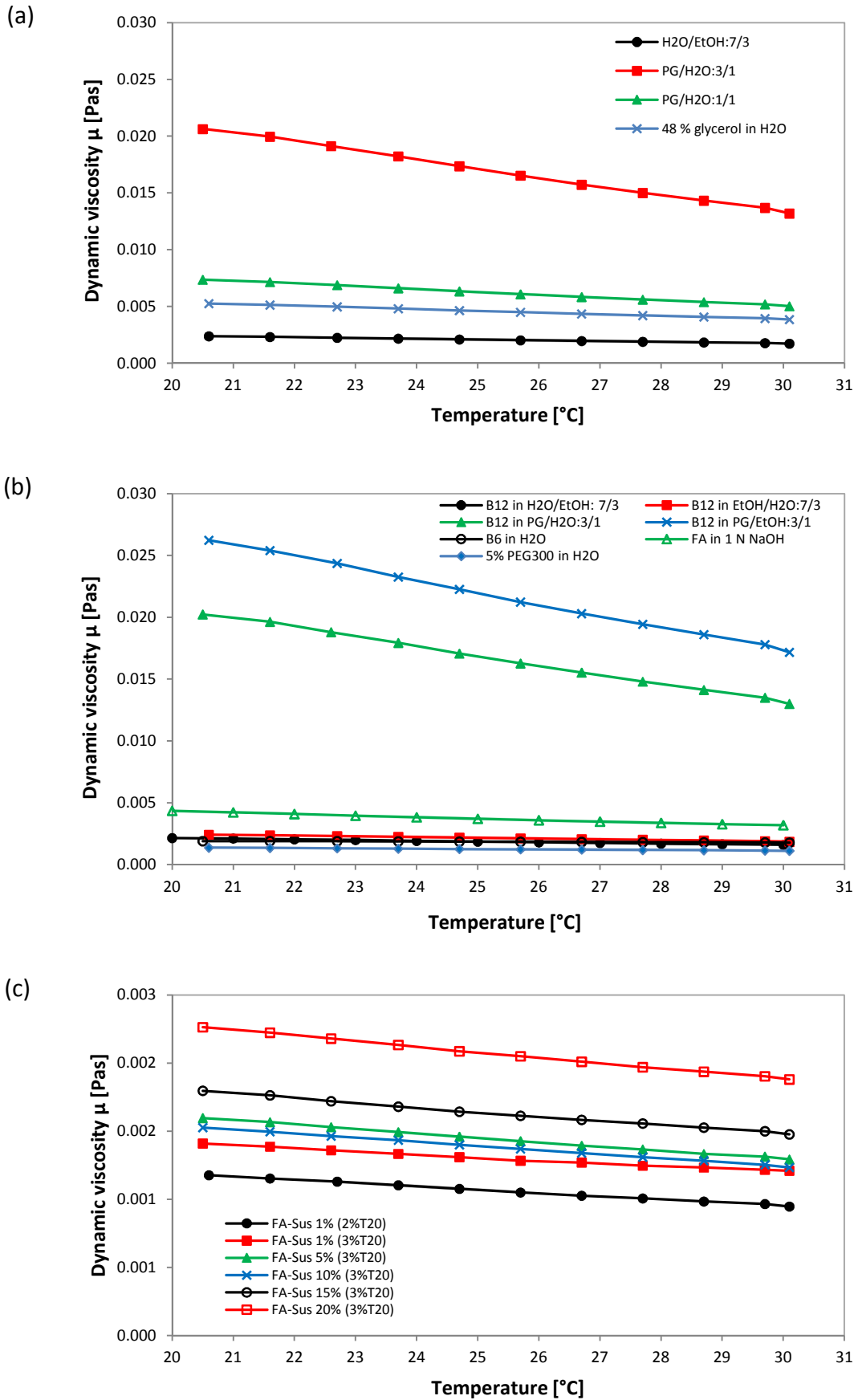


Figure 15: : Dynamic viscosity of (a) solvent mixtures, (b) solutions and (c) FA suspensions for a temperature range of 20 - 30°C at the constant shear rate of 500 s^{-1} .

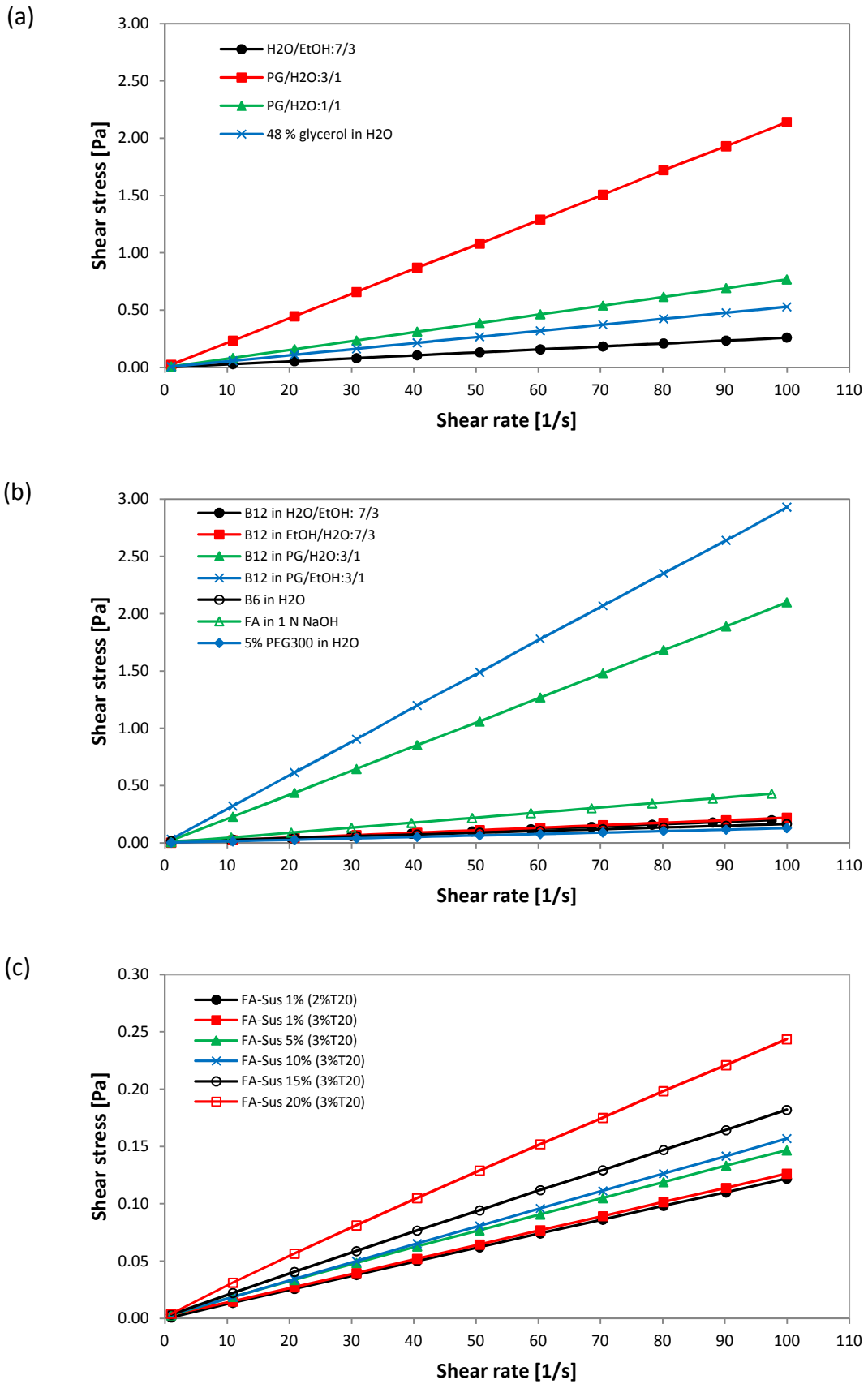


Figure 16: Flow curves of the same liquids as in figure 15 measured at T = 20°C .

Figure 16 displays the flow curves of the same test liquids at 20°C. The shear rate was varied between 1 and 100 s⁻¹. Within this range, the flow curves of all tested liquids are linear functions, and thus all liquids are considered to be Newtonian.

However, a comparison of the dynamic viscosity at 100 s⁻¹ and 500 s⁻¹ (figure 17) shows for solutions containing B12 and EtOH and for the folic acid solution a significantly lower viscosity at 500 s⁻¹. This could indicate shear thinning behavior due to solvation effects.

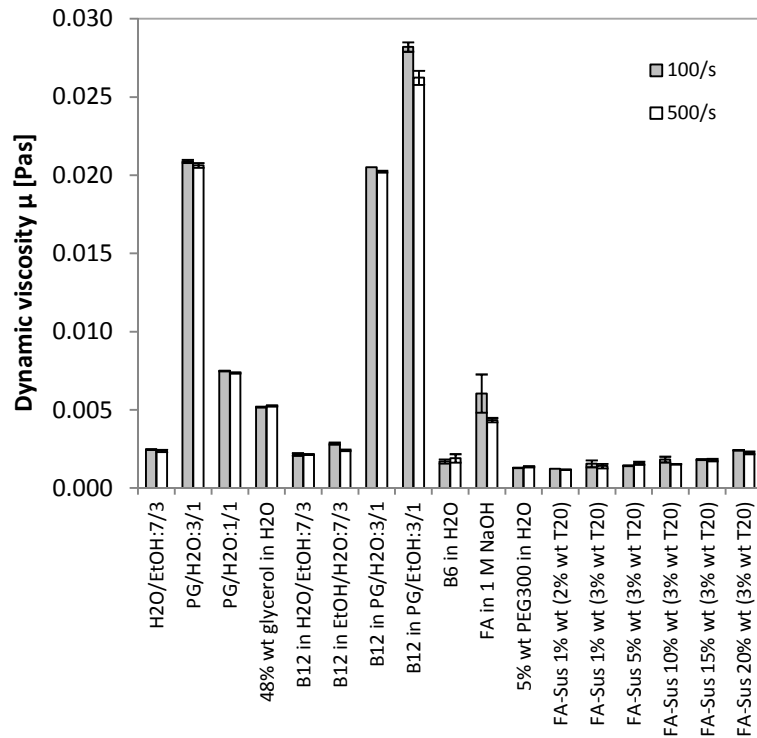


Figure 17: Comparison of the dynamic viscosities measured at shear rates of 100 s⁻¹ and 500 s⁻¹ at 20°C.

5.1.2 CONTACT ANGLE

To obtain information about wetting phenomena at the nozzle orifice, the three phase contact angle between air, glass and test liquid was measured. Wetting at the nozzle orifice can lead to the formation of a thin liquid film which can interfere with the droplet formation process, resulting in deflections of the ejected fluid jet and an increase in energy required for ejecting droplets [14].

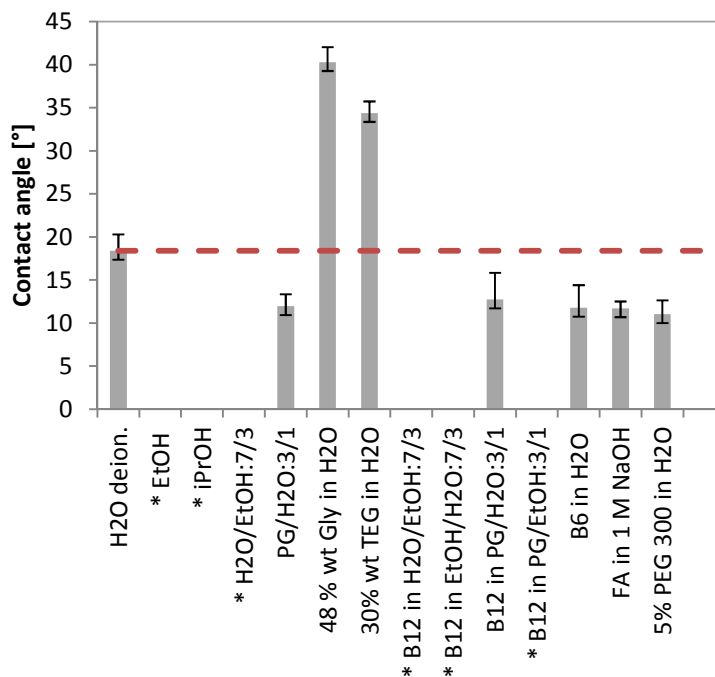


Figure 18: Contact angle [°] of investigated liquids. All liquids marked * showed immediate wetting of the glass surface. The red dashed line indicates the contact angle of water on glass.

Figure 18 shows the contact angle of the test liquids on a glass substrate. The highest contact angle was found for the glycerol/water mixture, and the lowest for the polymer solution. For pure solvents, mixtures and solutions containing solvents, as well as suspensions containing a surfactant, no contact angle on glass could be determined due to complete wetting of the test surface. In these cases the contact angle is practically zero.

In extreme cases, liquids showing complete wetting slowly leak out of the ejection aperture, so that droplet formation is prevented entirely. This behavior can be suppressed by applying a sufficiently high negative internal pressure inside the glass capillary. In the conducted drop formation experiments, usually a negative pressure of 10 mbar was enough to avoid leaking. For folic acid suspensions with 1% wt FA and variable content of surfactant (1-3% wt tween 20) the negative internal pressure had to be set as high as 50 mbar to enable droplet formation. Once the process was established, however, the negative pressure could be lowered to 10 mbar. This could be due to the fact that the surface active properties of surfactants depend on the diffusion of surfactant molecules to the freshly formed liquid surface. Since the DOD droplet formation in general occurs faster than diffusion, equilibrium

surface tension conditions are not obtained and therefore the surface tension of the aqueous suspension is closer to that of pure water [41][42].

5.2 DROP-ON-DEMAND DROPLET EJECTION

The results presented in the following section are intended to illustrate the development of pharmaceutical test fluids that are suited for the application of APIs on paper carriers.

5.2.1 VITAMIN SOLUTIONS

Vitamin B6 dissolved in pure water was very hard to work with. Monodisperse droplets were achievable. However, B6 showed a tendency to recrystallization, both within the nozzle and on the nozzle orifice. This resulted in a deviation of the ejected droplets and, when the crystals were large enough, in complete blocking of the nozzle. In these cases, the process could not be restarted again, and the drop generator had to be cleaned thoroughly. There was no explanation found as to why B6 would recrystallize in one experiment and not in another. But even when B6 was dissolved properly, problems with droplet ejection occurred. An unstable liquid meniscus would sometimes break up into smaller secondary droplets when it was not retracted back into the nozzle. This behavior led to fluid deposition on the nozzle aperture which then caused directional instabilities. For bigger droplets, the direction of ejection was not perpendicular to the nozzle plate. In addition, ejection velocity jitter was observed.

Folic acid was dissolved in 1 M NaOH to react to a neutral solution of sodium folate. This liquid produced monodisperse droplets for pulse widths between 21 and 25 μs and required a drive amplitude of at least 100 V. The best drop formation characteristics were found between 100 and 500 Hz, but monodisperse droplets were also observed for ejection frequencies of up to 2000 Hz. Drive settings were reproducible and did not shift when the ejection rate was changed. One problem observed was fluid build-up on the aperture face that caused an angular deviation of the fluid jet. To avoid droplet deflection it was necessary to wipe the nozzle aperture regularly. Also, adjusting of the drive voltage amplitude improved directional accuracy.

After a period of non-ejecting, the sodium folate partly recrystallized in the capillary and formed clogs that had to be removed before the ejection process could be resumed. This was usually achieved by flushing the glass capillary with test liquid.

The first attempt to create a jettable B12 solution was to dissolve B12 in a mixture of H₂O and EtOH with a volume ratio of 7/3. The liquid produced monodisperse droplets for pulse widths between 15 and 17 μ s. The droplets were small and were ejected perpendicular to the nozzle orifice. A second pulse width range that produced stable, monodisperse droplets was found between 24 and 30 μ s for ejection rates up to 1 kHz. The directional stability of these droplet streams, however, was not as good. The drop formation process appeared to be more reliable for ejection rates > 200 Hz. Excess drive amplitude tended to cause spray formation. At some settings, ejection velocity jitter was observed. It was necessary to adjust the negative internal pressure frequently, which could be an indication for the formation of air bubbles in the glass capillary. The restart after a period of non ejection was good though. In an attempt to improve the ejectability of B12, the volume ratio of the mixture was inverted to 7 parts EtOH and 3 parts H₂O. Stable drop formation was found for pulse widths between 28 and 35 μ s for ejection rates up to 400 Hz. Reproducibility was not very good, as some settings produced monodisperse droplets in one experiment and satellites in another. The drive settings changed with changing ejection rate. It was crucial to find the correct drive amplitude for a certain pulse width, because small deviations from it could disturb drop formation. In some cases, the droplets were ejected at an angle not perpendicular to the nozzle aperture. This solvent mixture containing more alcohol than water did not show better drop formation than the mixture with the inverted volume ratio. Therefore, the examination of this liquid was not further pursued.

After the promising ejection test of PG/H₂O:3/1, which was suggested as a reliable test liquid by Lee a new DOD system [14], B12 was dissolved in this mixture to determine if this improved its ejection properties. This liquid showed the best drop formation characteristics of all tested vitamin solutions. Stable, monodisperse droplet ejection was observed for a wide range of drive settings. Monodisperse droplets were easily achieved for pulse widths between 25 and 35 μ s and up to ejection rates of 4 kHz. The drive settings did not change with increasing ejection rate and were highly reproducible. Excess amplitude did not cause spray formation, but rather the elongation of the liquid filament ejected from the nozzle. The liquid portion usually fragments into secondary droplets that may merge with the

primary droplet or remain separated, depending on the applied drive amplitude. The directional accuracy was good, and no velocity jitter was observed. High ejection rates (> 3 kHz) required an increase in drive amplitude. The restart behavior was excellent.

To determine if similar or even better drop formation could be achieved, H₂O was exchanged for EtOH in the solvent mixture, while the volume ratio and the B12 concentration were kept the same. B12 did not as readily dissolve in this mixture as in PG/H₂O:3/1 and thus required longer stirring. Monodisperse droplets were generated for pulse width between 25 and 30 μ s and required an increase in drive amplitude in comparison to the mixture with water. Stable, satellite free droplets were observed at ejection rates as high as 5 kHz.

5.2.2 POLYMER COATINGS

An additional aspect in this study was to investigate the possibility of dispensing protective coatings on paper substrates using a DOD droplet generator. The general idea was to overprint API deposits with polymer dispersions or solutions producing a dense protective film. This polymer film not only protects the API from exposure to air and moisture, but may also allow for application of multiple drugs separated by barrier layers. By applying special polymer layers it is even possible to control drug delivery. Polymers with pH dependent dissolving characteristics can release a drug over an extended period of time or enable delivery of active ingredients to specific areas of the intestine.

To benefit from both extended release and protective properties, two acrylic materials typically used for this purpose in tablet coating, Eudragit L 100-55 and Eudragit E 100, were selected for this study. Eudragit L 100-55 only dissolves at a pH higher than 5.5 and is therefore resistant to gastric fluids. It is often used for enteric formulations. Eudragit E 100 is soluble in gastric fluid up to (pH 5.0) but not in saliva. Thus it is often applied to mask unpleasant tastes of pharmaceutical ingredients.

In tablet coating, Eudragit polymers are usually applied as aqueous dispersions rather than organic solutions. Compared to polymer solutions, dispersions exhibit more favorable rheological and film formation properties. Therefore Eudragit L 100-55 was first tested in its commercially available enteric formulation (trade name L 30 D-55), which is an aqueous dispersion with 30% wt particle content. The dispersion was used undiluted, and no process additives like plasticizers or pore formers were added. Neither the dispenser head, nor the

liquid reservoir was heated to avoid evaporation of dispersion medium and clogging of the nozzle orifice.

The results of the dispensing tests are displayed in figure 19.

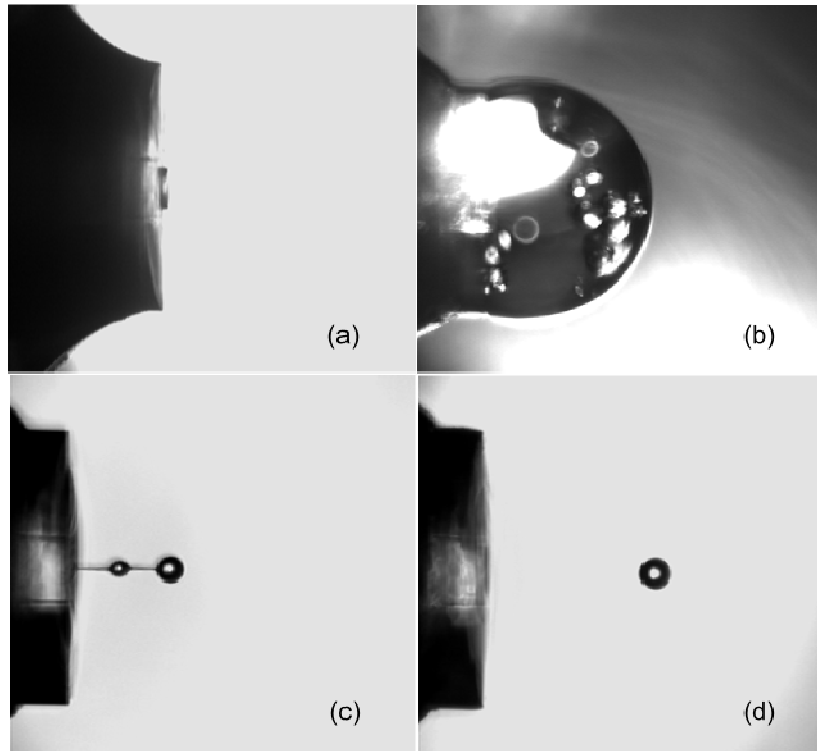


Figure 19: Results of polymer coat dispensing. (a) 30% wt Eudragit L 30 D-55 dispersion, (b) 15% wt Eudragit L 100-55 in ethanol, (c) 1.5% wt Eudragit L 100-55 in ethanol and (d) 1% wt Eudragit E 100 solution in isopropyl alcohol/acetone/H₂O.

As soon as the droplet dispenser was activated, the 30% wt Eudragit L 30 D-55 dispersion formed a solid plug that clogged the capillary completely (figure 19a). The plug could neither be jetted out by applying pressure to the reservoir, nor disintegrated in ultrasonic cleaning mode (application of actuation frequency of 12 kHz). Apparently the high shear stress inside the capillary during the dispensing process can cause coagulation of the dispersed latex particles, thus blocking the nozzle [43].

Since Eudragit L 100-55 is soluble above pH 5.5, the capillary had to be filled with alkaline solution (1 M NaOH) and extensively rinsed with water afterwards.

To avoid further coagulation of particles, the polymers were dissolved in organic solvent. Therefore a concentrated Eudragit L 100-55 solution containing 15% wt of polymer in pure ethanol was prepared for dispensing. Figure 10b shows a gel-like mass protruding from the print head during the dispensing process. The clear paste was probably developed due to

rapid solvent evaporation at the nozzle orifice turning the solution to be too viscous for proper jetting.

The same polymer solution was further diluted to 1.5% wt polymer content and filled into the dispenser.

Figure 19c shows 1.5% wt Eudragit L 100-55 in ethanol ejected from the nozzle. Microdrop formation was possible at operation settings of 200 Hz, 100 V and 28 μ s. The diluted polymer solution exhibited a rather interesting filament break up. The satellite droplet was neither sucked back into the dispenser nozzle, nor into the primary droplet. The main and satellite drops were formed separately to recombine after a short flying time.

Nevertheless, the drop formation itself was rather unstable, because the generated droplets tended to burst easily into two or more droplets when subjected to vibration. During the process, a gel-like residue built up at the nozzle orifice that seriously disturbed droplet formation (figure 20). Also pulse amplitude and width had to be increased over time to continue dispensing. Furthermore, the polymer solution starts to thicken quickly as soon as the process is interrupted. After a downtime of 10 to 15 minutes, the drop formation can hardly be resumed without cleaning the nozzle first.

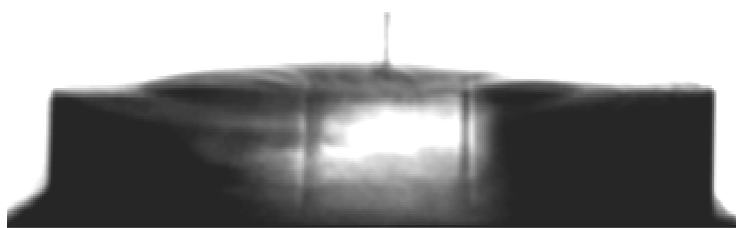


Figure 20: Enhanced image of Eudragit nozzle build up. Film formation seriously disturbs droplet generation.

The formation of monodisperse droplets was also achieved with 1% wt Eudragit E 100 in a mixture of isopropyl alcohol, acetone and water. In comparison to 1.5% wt Eudragit L 100-55 in EtOH, the generated droplets seemed to be more stable and less inclined to burst (fig. 10d). Dispenser parameters were set to 200 Hz, 100 V and 41 μ s. However, the driving voltage also had to be adjusted over time, and the glass capillary clogged when the process was stopped for more than 10 minutes. In addition, indications of new polymer build-up inside the nozzle have been observed during the process.

In conclusion, dispensing of polymers is possible with the microdrop system, but only for dilute solutions. The process is unstable and the glass capillary prone to clogging. A major

disadvantage of this application of coating is the necessity for harsh chemicals to remove the polymer residues inside the nozzle and on the nozzle surface. Although Eudragit L 100-55 dissolves readily above pH 5.5, a strong alkaline medium like NaOH is needed to remove it thoroughly. For Eudragit E 100, however, extensive rinsing with organic solvents was sufficient. But even that would be undesirable for an implemented pharmaceutical process. In addition to complications during drop formation it remains unclear if dense protective films can be formed on a porous substrate like paper. Aqueous latex dispersions, for example, are known for their disturbed film formation on porous surfaces [43]. It is conceivable that this is also true for polymer solutions applied to very rough and inhomogeneous surfaces like the uncalendered and uncoated paper substrates used in this study. Moreover, elution or redistribution of the active pharmaceutical ingredient is likely when dry API deposits are overprinted with coating solutions containing organic solvents. Considering the possible damage of the printhead, it is advisable to explore other coating techniques for this purpose.

5.2.3 FOLIC ACID SUSPENSIONS

One of the main issues in the development of formulations for inkjet printing is solubility of the payload. In general it is preferable to maximize concentration, because, the higher the concentration of the solution, the less liquid has to be deposited on the substrate to achieve a certain dosage. This is especially important because the paper substrates are limited in their absorption capacity. In addition, printing time can be considerably shortened by using highly concentrated solutions. Unfortunately many drug substances are poorly or not soluble in water or solvents approved for pharmaceutical use. Such APIs can be suspended in a carrier fluid for ejection with a DOD droplet generator.

Folic acid is almost insoluble in water and most solvents. Thus, it was selected as a test substance to demonstrate that insoluble drugs can be formulated as suspensions and ejected with an inkjet printing system. In order to prepare stable nanosuspensions, the particles should be small enough not to settle gravitationally. This is usually achieved through a particle diameter of less than 1 μm . In addition, fractured particles should be completely wetted by the suspending medium to suppress reagglomeration [14]. Therefore, a surfactant is added to the dispersion medium as a stabilizing agent. Via preliminary contact

angle measurements Tween 20 was determined as a suitable stabilizer because of its high affinity towards folic acid [44].

Preparing the suspensions, folic acid content and surfactant content were varied between 1 and 20% wt and 1 and 3% wt, respectively. Table 11 gives an overview of the used dispenser settings and the resulting drop diameters.

| FA content [%] | Surfactant [%] | Frequency [Hz] | Amplitude [V] | Pulse width [μ s] | Drop diameter [μ m] |
|----------------|----------------|--------------------------------------|---------------|------------------------|--------------------------|
| 1 | 1 | no stable droplet formation observed | | | |
| 1 | 2 | 100-400 | 87-104 | 18-31 | 54-72 |
| 1 | 3 | 100-300 | 90-100 | 25-30 | 62-69 |
| 5 | 3 | 100-600 | 85-100 | 25-30 | 51-65 |
| 10 | 3 | 100-3000 | 93-115 | 25-30 | 56-84 |
| 15 | 3 | no stable drop formation observed | | | |
| 20 | 3 | no stable drop formation observed | | | |

Table 11: Investigated operation regions and resulting droplet diameters of suspensions with varied folic acid and surfactant content. Percentages refer to weight percent.

The suspensions containing 1% wt FA showed different ejecting behavior, depending on their surfactant content. For 1% wt of Tween 20, stable drop formation could not be achieved. The fluid leaked out of the nozzle orifice, leaving a liquid film that burst into a chaotic spray as soon as the droplet dispenser was activated, although a strong negative pressure was applied. However, the suspension with 2% wt Tween 20 produced stable droplets within a frequency range of 100 to 400 Hz at more than one driving amplitude and pulse width setting. Applying the suspension stabilized with 3% wt surfactant allowed for the ejection of monodisperse droplets from 100 to 300 Hz. Interestingly, the window of operation settings within which drop formation was observed is significantly smaller than that of the 1% wt FA suspension with 2% wt surfactant.

The droplet ejection behavior improved significantly with higher folic acid content. A 5% wt content of folic acid with 3% wt Tween 20 allowed for stable droplet formation from 100 to 600 Hz for pulse widths of 25 and 30 μ s.

Even better results were achieved when the folic acid content was increased to 10% wt. Monodisperse droplets were observed for frequencies up to 3000 Hz within a certain range of pulse amplitudes (see figure 21).

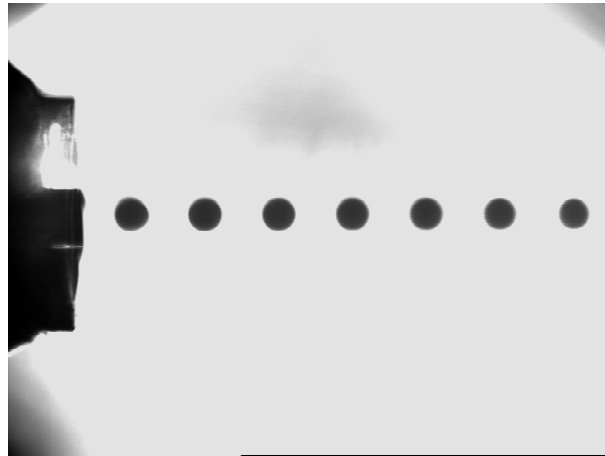


Figure 21: Drop formation of 10% wt folic acid suspension containing 3% wt Tween 20. Operating parameters were 2000 Hz, 93 V and 30 μ s. Drop diameter: 83.3 μ m

Figure 22 shows drop formation sequences of suspensions with 5% wt and 10% wt folic acid. The sequences are similar, apart from the fact that the droplet break-off from the liquid filament occurs slightly earlier for the 10% wt suspension. After droplet pinch-off, the liquid filament is retracted into the nozzle, while the droplet undergoes oscillating motions.

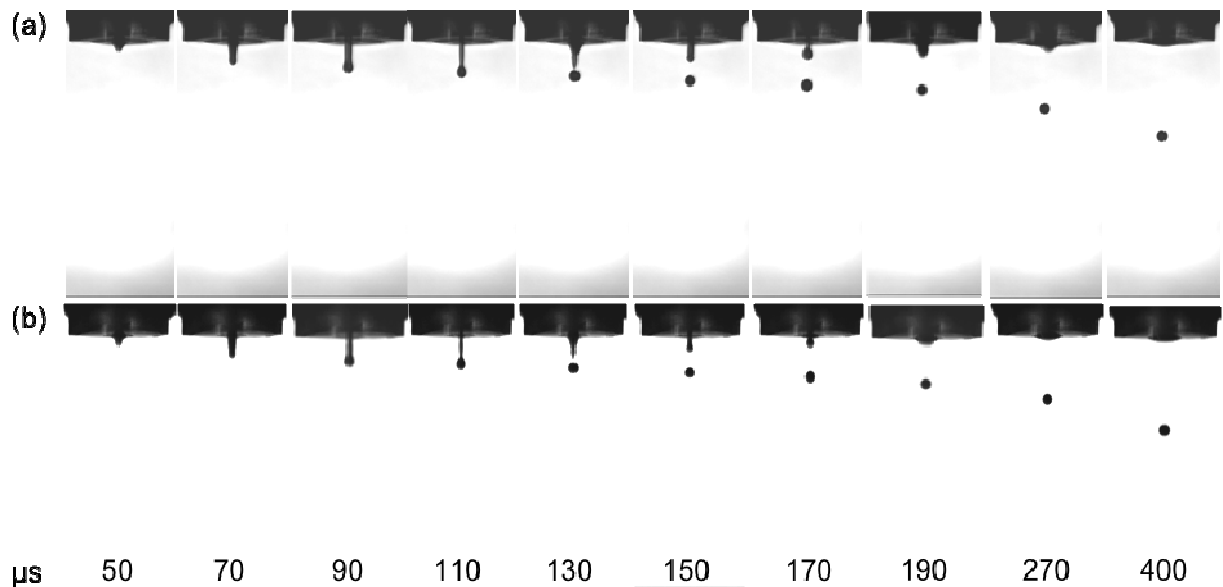


Figure 22: Droplet formation of (a) 5% wt and (b) 10% wt aqueous folic acid suspension containing 3% wt Tween 20. Time in μ s corresponds to illumination delay relative to actuation signal. Operating parameters were 200 Hz/94 V/25 μ s and 200 Hz/100 V/25 μ s, respectively.

One reason for the improved droplet ejection performance could be the more favorable wetting characteristics of suspensions with higher payload content during operation. Although in both cases partial wetting of the nozzle occurred the process was stable and reproducible. The liquid film formed at the nozzle orifice tends to be smaller the higher the folic acid content (see figure 23), thus the drop formation is less disturbed than for 1% wt FA suspensions.

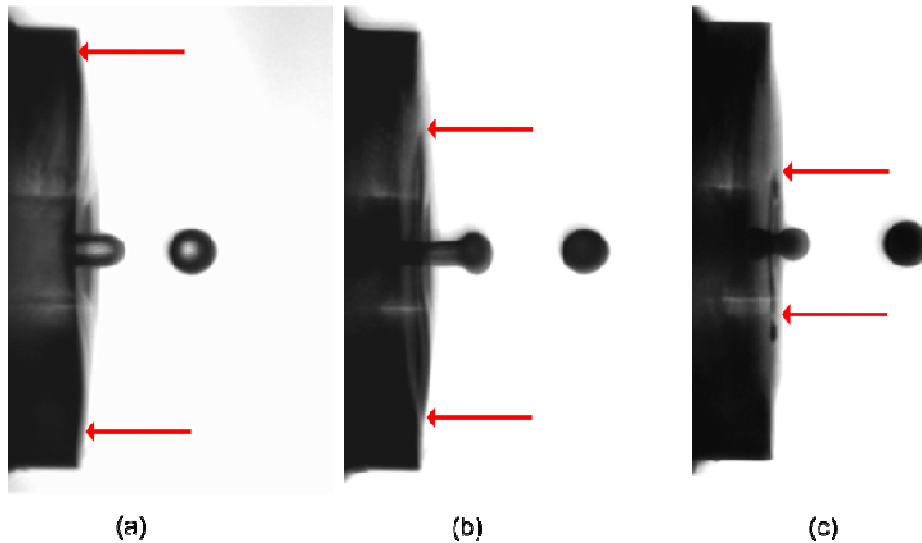


Figure 23: Visualization of nozzle wetting of different suspensions. (a) 1% wt, (b) 5% wt and (c) 10% wt. Applied operating parameters were 200 Hz, 25 μ s and 94 V for (a) and (b), and 100 V for (c). Red arrows show boundary of nozzle surface wetting.

For suspensions with a folic acid content of 15% wt or higher, generation of stable droplets was not observed. The capillary was frequently blocked by coagulating particles deposited inside the nozzle and on the nozzle surface, which produced a chaotic spray of randomly sized droplets.

5.3 DROP FORMATION PROCESS

The present section is dedicated to the results and discussion of DOD droplet formation. First of all, the ejectability of the investigated liquids is discussed in terms of fluid properties. Then the different stages of droplet formation are presented by means of 3 different liquids. Finally, the dependency of drop diameter and velocity as functions of operation parameters is demonstrated.

In figure 24 the investigated liquids are displayed in a surface tension vs. dynamic viscosity diagram which was borrowed from Dorfner [45]. Considering their ejectability with the used DOD system, the graph can be divided into three regions. Note that the σ boundary line is based on empirical results, whereas the μ boundary line is estimated. Region (I) is governed by comparably high surface tension and low dynamic viscosity and consists of the test liquids that showed poor DOD drop formation. Fluid ejection tests showed that these liquids were ejectable only within a small range of operating parameters and tended to satellite or spray formation. Liquids belonging to region (II) exhibited good ejectability and were more tolerant towards a change in operating parameters, with the exception of suspensions with high FA content (15 and 20% wt). According to their physical properties they also belong to region (II) but are hardly or not at all ejectable with this system due to their high particle concentration. Region (II) is characterized by a moderate surface tension and relatively low viscosity.

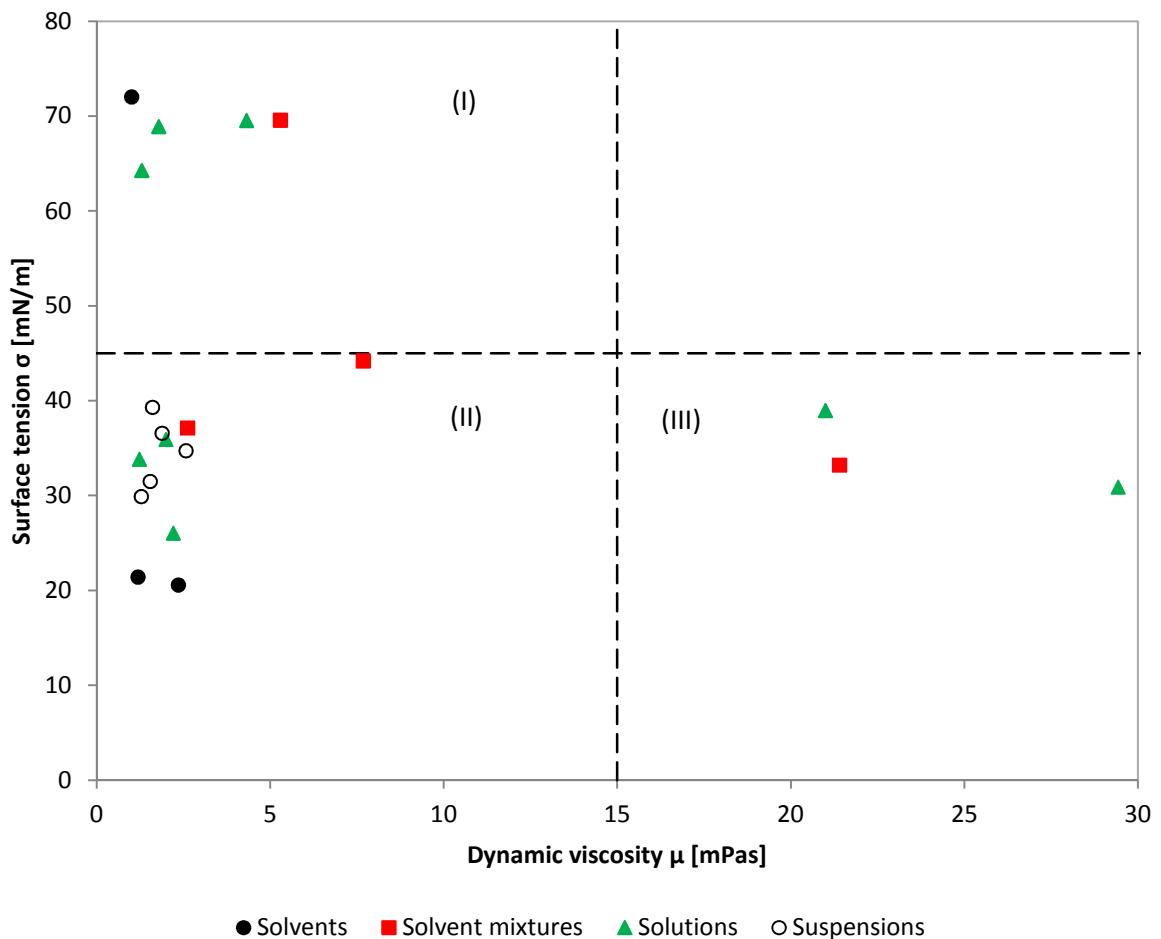


Figure 24: Surface tension [mN/m] vs. dynamic viscosity [mPas] of investigated liquids (adapted from [45]).

Region (III) contains three liquids showing the most stable and consistent drop formation. This area is governed by a moderate surface tension and, for ink-jet printing a relatively high dynamic viscosity. With these liquids the droplet generation was remarkably reproducible and stable against ambient conditions. At high actuation amplitudes, where usually spray formation occurs, only the stretching of highly elongated liquid filaments was observed.

Figure 25 illustrates the stages of drop formation for three liquids with considerably different liquid properties. According to the categorization presented in figure 24, each of these liquids belongs to a different ejectability region. The first shown liquid is H₂O (region (I)), the second PG/H₂O:3/1 (region (III)) and the third a 10 % wt FA suspension (region (II)). In the first series of images (figure 25a), a tapered liquid thread emerges 50 μs after the actuation signal was applied. The liquid thread first elongates, adopts a bulbous shape and then necks at the back of the drop. The result is a primary drop that breaks off from the remaining filament. The now free liquid filament is retracted back into the nozzle, where it dissipates the rest of its energy by oscillations of the fluid meniscus at the nozzle orifice. The free primary droplet also shows excessive oscillation.

The second series of images (figure 25b) shows the typical drop formation of a high viscosity liquid. Here the liquid filament also starts as a tapered liquid portion, but it is then stretched to a longer liquid column. This liquid column also forms a bulbous head like water, but the necking of the liquid portion starts at the nozzle exit and not at the backside of the droplet. Finally the liquid portion pinches off at the nozzle orifice, and the tail is recoiled into the primary droplet.

The drop formation of the third liquid presented (FA suspension) shows elements of both previously discussed ejection mechanisms. The liquid filament extends further than for water, but the droplet break-off also occurs at the back of the droplet, and not at the nozzle orifice. Interesting in this case is also the shape of the retracting liquid column after pinch-off of the primary droplet. The retracting fluid portion shows additional constraints (130 μs after actuation signal), which do not result in a secondary break-off, but rather in the formation of a suspended droplet that is sucked back into the capillary.

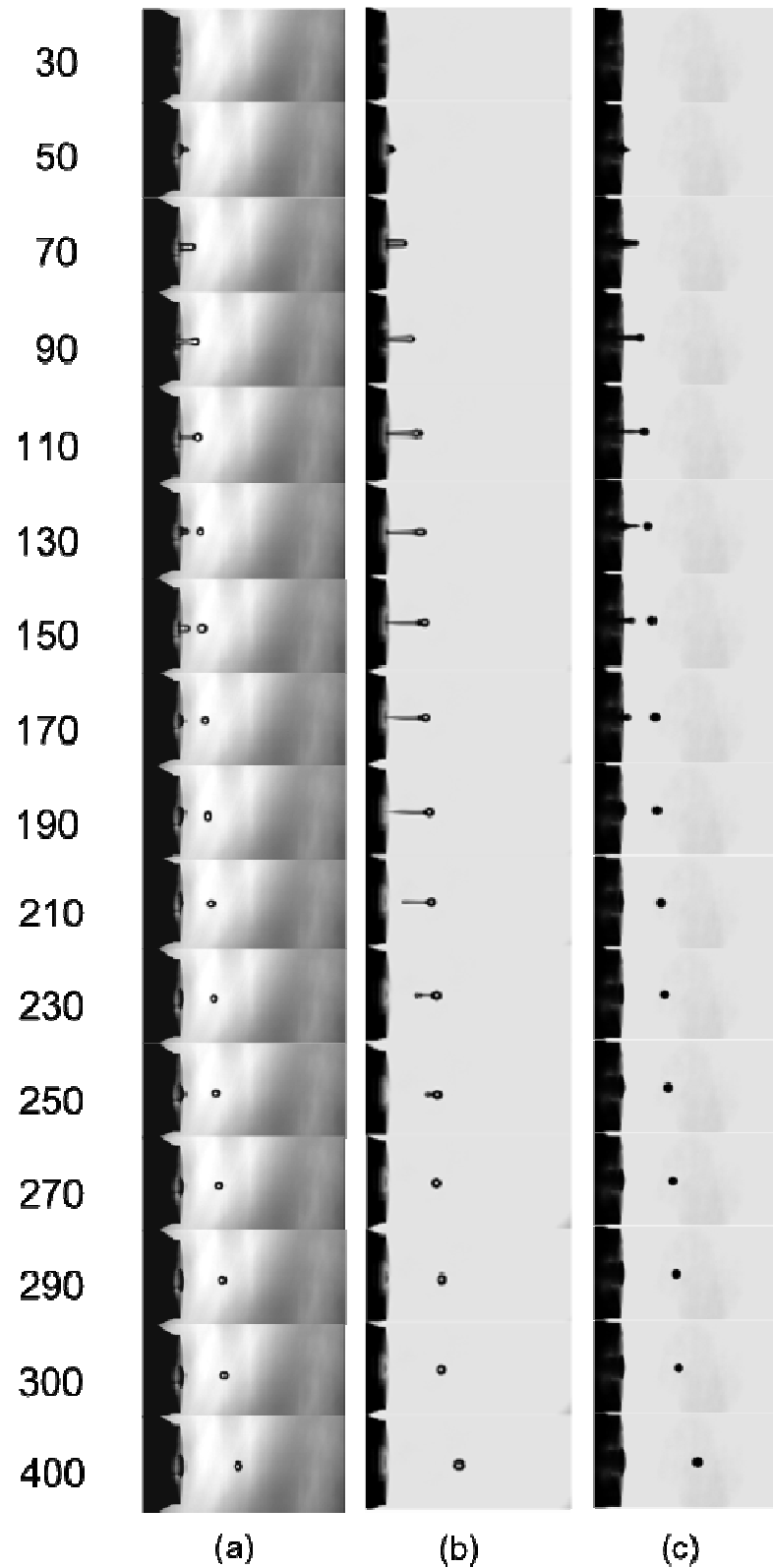


Figure 25: Drop formation of three different test liquids. (a) H₂O HPLC grade at 100 Hz/100 V/25 μs, (b) PG/H₂O:3/1 at 200 Hz/120 V/25 μs, (c) 10 % wt FA suspension at 200 Hz/100 V/25 μs. The numbers on the left indicate the time after start of the actuation signal in μs.

The following section is concerned with the dependency of drop size and velocity on operating parameters of the droplet ejector. Four liquids were selected to measure drop size and velocity as functions of actuation frequency, driving voltage and pulse width. In each experiment, two of the three parameters were kept constant, while one was varied. The results of these measurements are presented in figure 26 and figure 27.

The drop diameter decreases with increasing frequency until about 400 Hz (figure 26a). After that it remains almost constant for PG/H₂O:3/1 and the glycerol/water mixture. For PG/H₂O:1/1 the drop diameter shows an increase for frequencies greater than 400 Hz. For EtOH no values exceeding 400 Hz could be obtained due to increasingly unstable drop formation.

The variation of the drop diameter with pulse width shows a steady rise until 25 μ s followed by a slight downward trend (figure 26b). Between 25 and 35 μ s, the drop diameter remains almost constant for the PG and glycerol mixtures. For EtOH only three values could be obtained.

Generally the drop diameter increases not only with increasing pulse width, but also to a certain extent with increasing pulse amplitude. As shown in figure 26c, the PG/H₂O mixtures show an initial rise in drop diameter. The mixture with the lower viscosity PG/H₂O:1/1 shows a maximum at 100 V, whereas the high viscosity mixture shows a maximum at 124 V, followed by a minimum at 130 V. For the glycerol - water mixture, a steady increase in drop diameter was found, whereas for EtOH an inverse trend was observed.

Figure 27 displays results of the droplet velocity measurements. The influence of the dispensing frequency on drop velocity is small. At low frequencies, the velocity remains almost constant, whereas at higher frequencies the velocity seems to oscillate around a constant value. These oscillations are more pronounced for liquids with lower viscosity.

For the drop velocity as a function of pulse width, no obvious trend was found. A first increase in drop velocity between 15 and 20 μ s followed by a decrease was observed. A second increase was found around 35 μ s.

The pulse amplitude, however, showed a linear relation with the drop velocity. From this plot, the minimum driving voltage was obtained for the 4 liquids by means of extrapolation. This minimum signal amplitude (ΔU^*) is required to produce drop velocities greater than 0. The thus derived ΔU^* are 104.4 V, 80.7 V, 89.5 V and 73.3 V for PG/H₂O:3/1, PG/H₂O:1/1, glycerol in H₂O and EtOH, respectively.

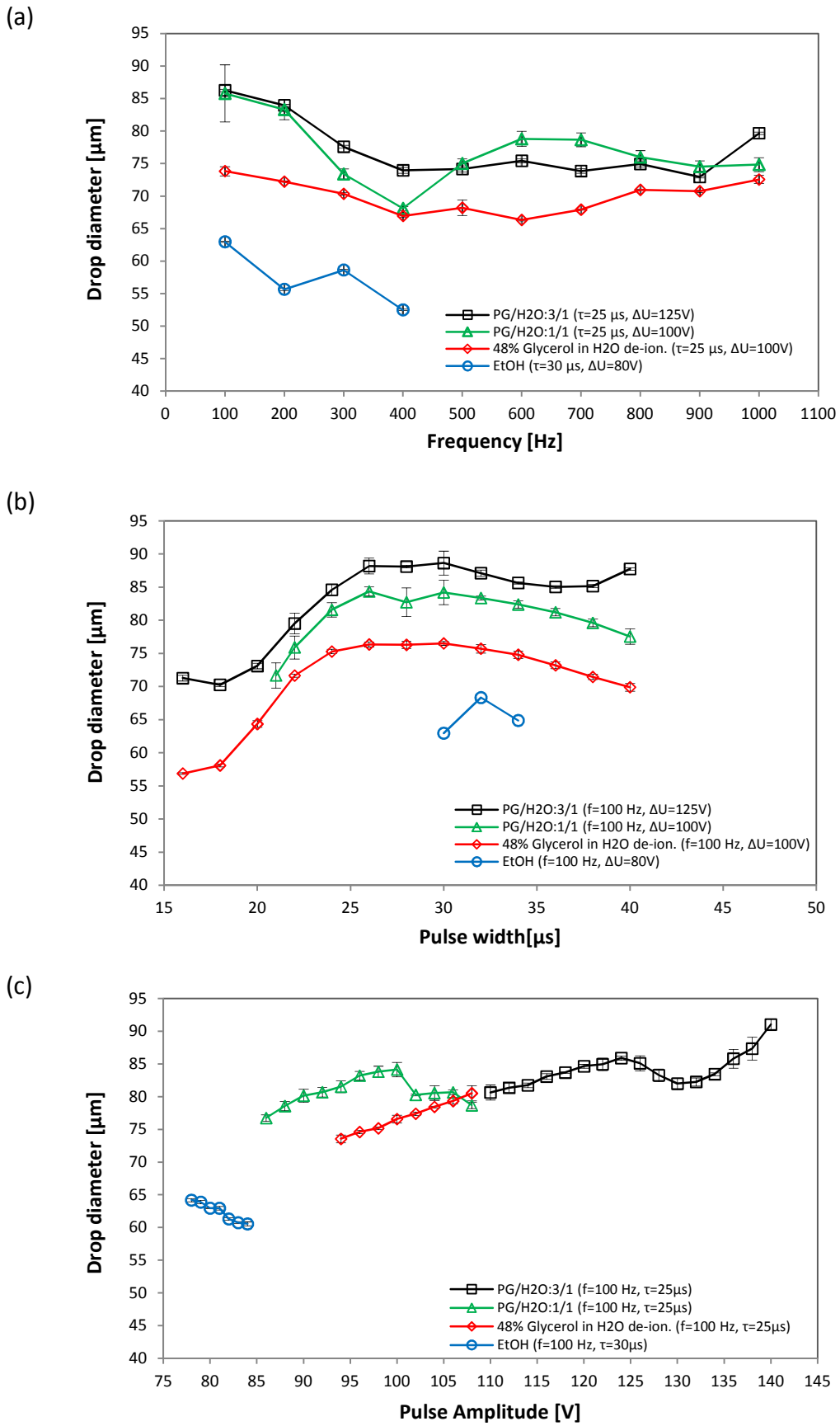


Figure 26: Drop diameter vs (a) frequency, (b) pulse width and (c) pulse amplitude.

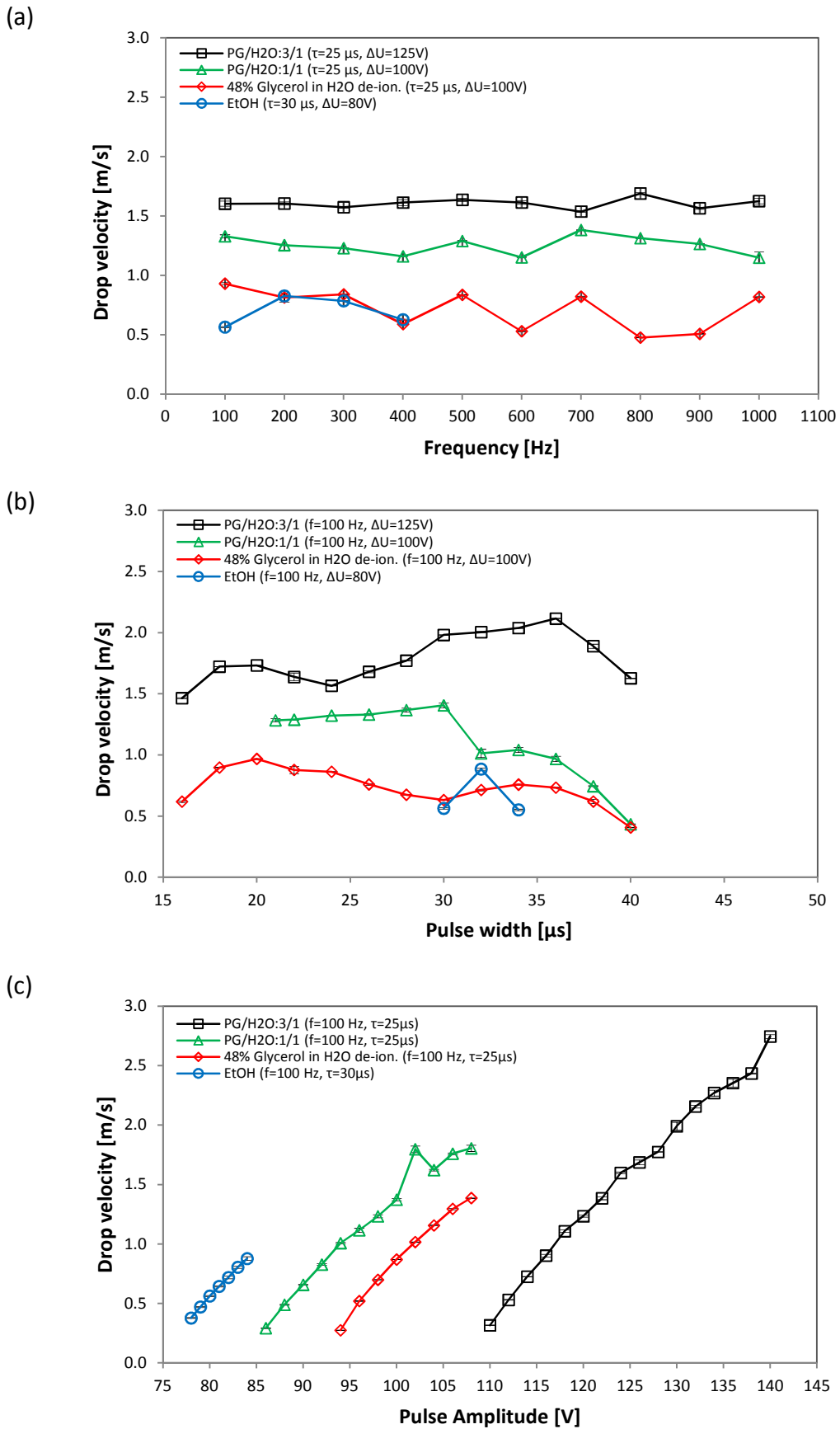


Figure 27: Drop velocity vs. (a) frequency, (b) pulse width and (c) pulse amplitude.

Considering this activation voltage, the velocity data can be represented as a function of the excess voltage ($\Delta U - \Delta U^*$) which is displayed in figure 28.

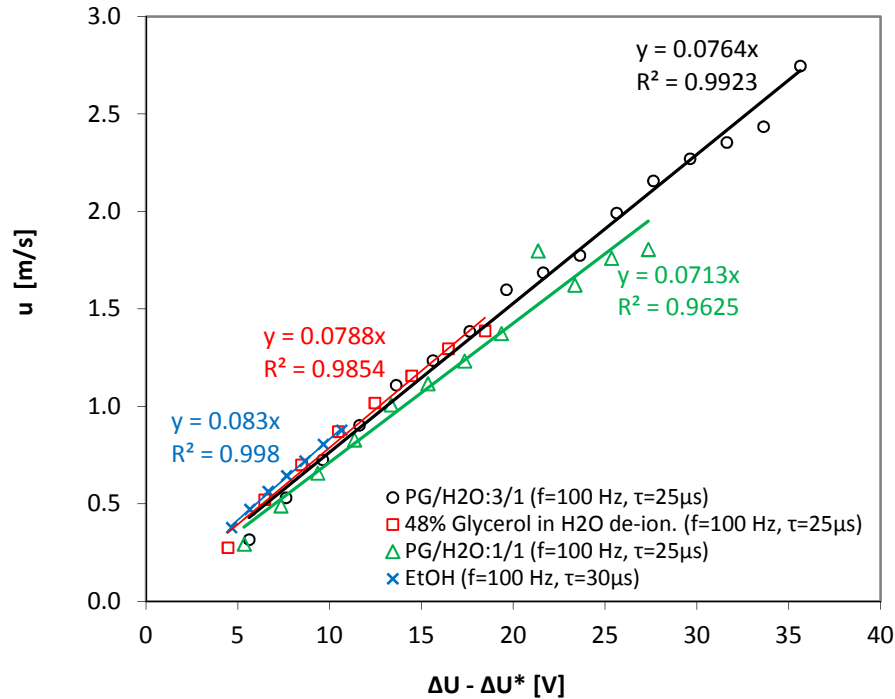


Figure 28: Variation of the droplet velocity with the excess voltage.

5.4 DOSING ACCURACY

One of the key features of the DOD inkjet printing process is its high reproducibility. It allows for accurate dosage of small amounts of substance and can therefore be a useful approach to deliver active pharmaceutical ingredients in precise and low doses.

For the most part of the present study, droplet volumes and diameters were determined using stroboscopically illuminated images. The calculation of the droplet diameter was based on finding the drop contour line by means of digital image processing algorithms. But automated boundary recognition processes can be biased by effects like drop oscillation or droplet flattening during flight and refraction [35]. By using a stroboscopic illumination source, the resulting image consists of several superimposed images of ejected micro droplets. Since these droplets are not always ejected to the exact same spot, the resulting drop appears to be larger than it really is. Krüger et al. found that the droplet volume they determined by optical means may be 1.17 times bigger than that determined by weighing.

They also found that the systematic error causing the optically measured droplet to appear bigger increases with increasing actuation frequency [46].

In addition to systematic errors due to superimposed droplet images, the light intensity of the illumination source increases with the actuation frequency, because the LED is synchronized with the actuation signal. This leads to overexposed images, on which the automated droplet contour determination is even more difficult. For these reasons it seemed prudent to verify the dosing accuracy by a second method.

To identify possible influences of fluid properties on dispensing accuracy, two liquids with considerably different viscosity and surface tension (H_2O and B12 in PG/ H_2O :3/1) were selected for these experiments. Both liquids were dispensed continuously and in bursts of 100, 1000 and 10000 droplets. Time stamped balance readings in 10s intervals were recorded using a balance printer. Between bursts and phases of continuous ejection the evaporation rate was observed. Since the experiment had to be conducted inside the balance housing, it was impossible to observe the droplets by optical means during the weighing experiments. Therefore the optical reference points were taken from another experiment for evaluation.

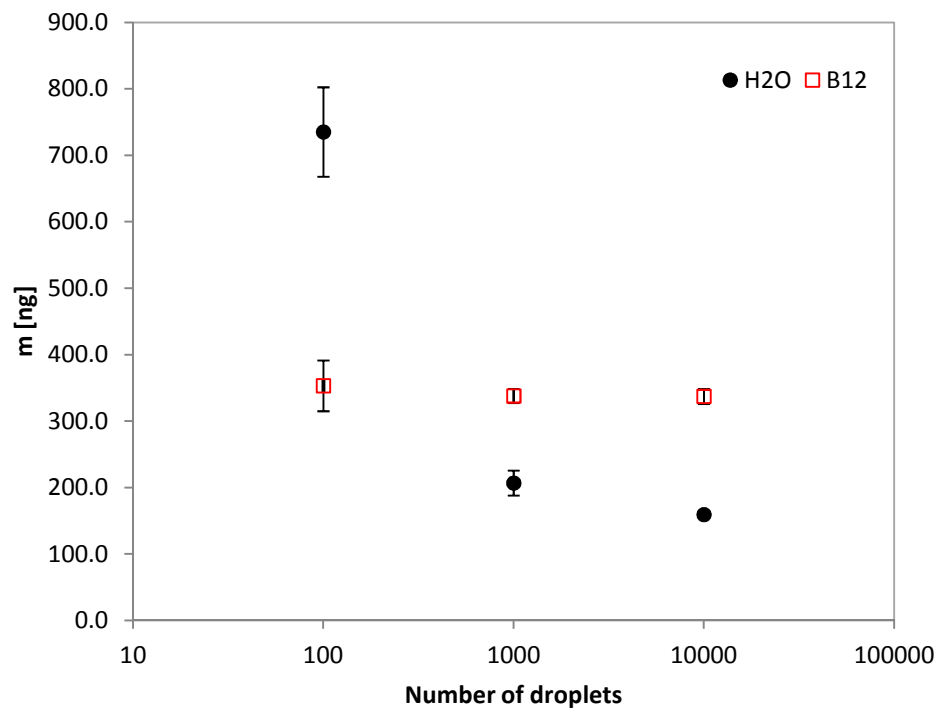


Figure 29: Average droplet mass in burst gravimetry. All droplet aliquots were dispensed in single bursts. All measurements were repeated at least 10 times. Operating parameters were 100 Hz / 100 V / 25 μs for water and 1000 Hz / 115 V / 30 μs for the B12 solution.

Figure 29 displays the results of burst gravimetry. For water the average droplet size seems to be more than 4 times higher in bursts of 100 droplets than in bursts of 10000 droplets. Since direct observation of the droplets generated in these experiments was impractical, it is impossible to determine the reason for the big difference in average droplet mass. It is reasonable to assume that the drop formation itself was unstable, thus producing satellite droplets or for some reason considerably bigger droplets in bursts of 100 droplets. Furthermore it appears that, the less droplets are ejected, the bigger the uncertainty, which is consistent with the findings of Verkouteren [35]. The obtained droplet masses for the B12 solution were similar for all three burst quantities, with the uncertainty again increasing with decreasing number of ejected droplets.

Table 12 shows the average droplet mass determined by continuous droplet gravimetry. Two runs were performed for each liquid and the average mass was calculated from at least 10 measurements.

| Liquid | Exp. | m [ng] | m STD [ng] | RSD [%] | m opt [ng] |
|------------------|------|--------|------------|---------|------------|
| H ₂ O | 1 | 358 | 13.5 | 3.8 | 218 |
| H ₂ O | 2 | 360 | 10.1 | 2.8 | 218 |
| B12 | 1 | 354 | 8.1 | 2.3 | 247 |
| B12 | 2 | 352 | 7.4 | 2.1 | 247 |

Table 12: Average droplet mass determined by continuous droplet gravimetry and standard deviation. Droplet dispenser settings were 100 Hz / 100 V / 25 μ s for water and 1000 Hz / 115 V / 30 μ s for the B12 solution.

As indicated by the low standard deviation the dispensing process shows good reproducibility for both liquids, which is apparently not the case in the burst mode. The masses of both H₂O and B12 solution droplets are quite similar, which means that the corresponding drop diameters are also within the same range (88 μ m and 86 μ m respectively).

The actual droplet mass was for both H₂O and the B12 solution higher than the mass derived from drop images (by 65% and 43%, respectively). This discrepancy is likely to be the result of limitations of the automated image processing. To allow for accurate drop contour determination it is necessary to convert the grayscale drop picture into a binary image. Therefore a threshold determining which pixels are classified as black (value 0) and white

(value 255) is computed from mean grayscale values in the original image. This means that the contrast between background and droplet should be maximized, but without overexposing the image. An overexposed image results in a poorly defined droplet edge as well. The light source in the used setup is coupled with the actuator signal. Thus, the illumination intensity is dependent on the dosing frequency and cannot be simply optimized for image analysis.

In figure 30 two examples of typical drop images of H₂O (left) and B12 in PG/H₂O:3/1 (right) are shown.

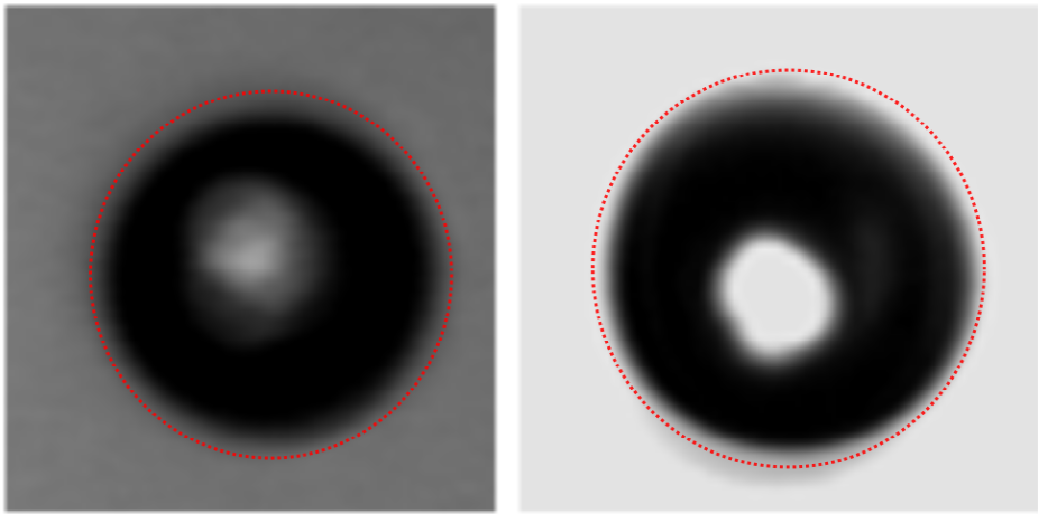


Figure 30: Enhanced droplet image of H₂O at a dispensing frequency of 100 Hz (left) and B12 solution at 1000 Hz (right). The red dotted line indicates the actual drop contour.

The image on the left was recorded at 100 Hz, showing poor contrast between drop and background. In the second image, recorded at 1000 Hz, the background is too bright to find the actual edge of the droplet. However, the dark red color of the B12 solution certainly adds to the contrast, which could be the reason for the smaller difference between optical and gravimetric method in this case. Nevertheless, the drop appears to be smaller than it really is.

5.5 DROP IMPACT AND SPREADING

The aim of these experiments was primarily to determine whether an ejected droplet is deposited or splashed on a macroscopically uneven, chemically heterogeneous surface like

paper. For printing of low dosage pharmaceuticals on paper, splashing would have considerable influence on dosing accuracy with possible cross-contamination and should therefore be avoided. For this series of experiments, the setup described in section 3.2.3 was used.

As mentioned in section 4.3, the outcome of a drop impact event depends mainly on the fluid properties of the used liquid, the impact velocity of the resulting droplet and the roughness of the substrate. The experimental setup did not allow for accurate measurement of the actual impact velocity, because the captured image section had to be minimized in order to maximize the frame rate of the high speed camera. Therefore initial velocities, which are measured after complete ejection of the primary droplet (procedure see section 4.2), were taken from another experiment to calculate dimensionless numbers important for the description of drop impact.

Four test liquids with considerably different characteristics were chosen to cover a wide range of fluid properties. Table 13 provides a summary of the applied test parameters.

| Liquid | H ₂ O de-ion. | B12 PG/H ₂ O:3/1 | FA in NaOH | FA-Sus (10% wt) |
|------------------------------------|--------------------------|-----------------------------|------------|-----------------|
| Frequency [Hz] | 30 | 100 | 30 | 30 |
| Pulse amplitude [V] | 100 | 120 | 110 | 100 |
| Pulse width [μs] | 25 | 25 | 25 | 27 |
| Mode | C | B | C | C |
| Drop diameter [μm] | 71.4 | 81.1 | 76.4 | 68.4 |
| Initial drop velocity [m/s] | 1.28 | 1.16 | 1.39 | 1.04 |
| We | 1.63 | 2.93 | 2.27 | 1.93 |
| Re | 91.5 | 4.70 | 26.3 | 45.5 |
| Oh | 0.014 | 0.364 | 0.057 | 0.031 |
| Density [kg/m³] | 998.25 | 1043.68 | 1073.46 | 1033.22 |
| Dyn. Viscosity [mPas] | 1.01 | 21.40 | 4.32 | 1.61 |
| Surface tension [mN/m] | 72.0 | 33.2 | 69.5 | 39.3 |

Table 13: Operating parameters, droplet characteristics and fluid properties. Drop diameter and initial drop velocity were measured @ 100 Hz. Initial drop velocity corresponds to velocity after droplet pinch off not to actual impact velocity. "C" and "B" refer to continuous and burst mode, respectively.

Each drop impact test was repeated at least 5 times on glass and four paper substrates. Figure 31 illustrates the drop impact results and droplet images up to 5 ms after impact.

Qualitative analysis of the captured images shows that in every test case the droplet was deposited on the substrate without any indication of break-up into secondary droplets. Contrary to expectations, fibers randomly sticking out of the surface of handmade papers (“TiO₂” and “CaCO₃”) do not promote droplet break up. However, they disturb the droplet trajectory enough to deflect the droplet away from its intended impact spot.

After deposition, the droplet either spreads until a maximum spreading diameter is reached, or it is absorbed immediately. In comparison to “TiO₂”, “CaCO₃” shows faster liquid absorption. On “H” and “Copy”, the droplet is rather evaporated than absorbed.

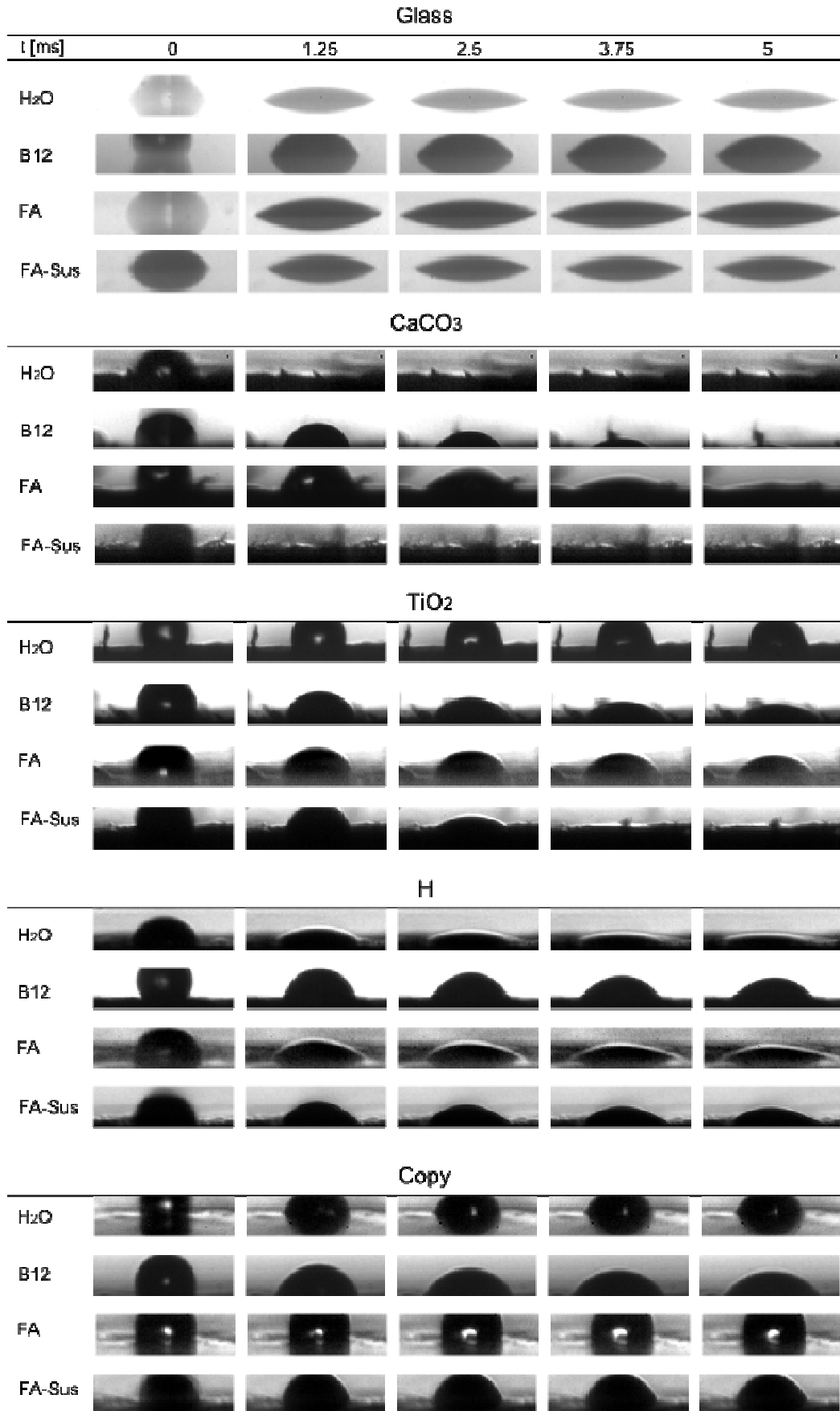


Figure 31: Drop impact of the 4 liquids in table 13 on glass and 4 paper substrates.

Furthermore, a mathematical model was applied to confirm complete deposition of all liquids on the used substrates. Mundo et al. found a correlation between Reynolds and Ohnesorge number that defines a distinct boundary between droplet deposition and splashing which can be expressed by eq. (5) [38].

$$K = Oh \cdot Re^{\frac{5}{4}} \quad (5)$$

According to the experimental results of Mundo et al. (1995), a liquid droplet is splashed above a K value of 57.7 and completely deposited below that value. This relation is only valid for Re formed with the drop velocity in the direction normal to the surface.

Figure 32 illustrates the relation between Ohnesorge and Reynolds number. The red line represents the boundary $K = 57.7$, dividing the graph into a splashing and a deposition region. The data points shown correspond to K numbers derived from all drop formation experiments conducted in this study. As already mentioned the Reynolds number was calculated using the measured initial velocity instead the actual impact velocity which was used by Mundo et al. This is rather a more critical case than is the real impact process, where the drop is slower due to aerodynamic deceleration.

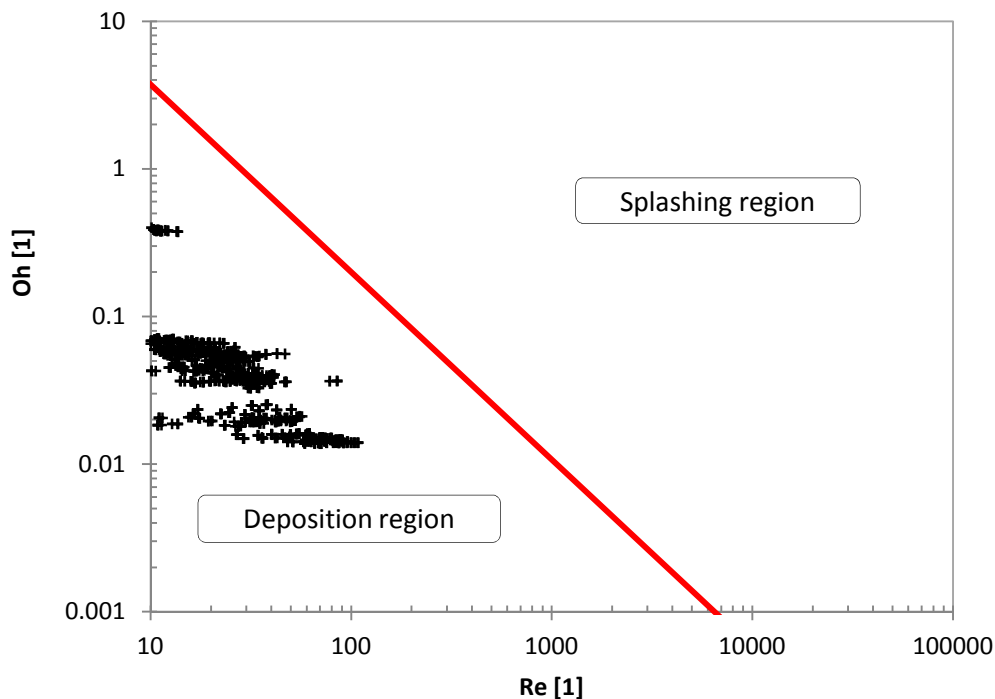


Figure 32: Impact monogram with boundary line between deposition and splashing regions as determined by [38].

As can be seen from the data shown above, all data points are well below the splashing limit. Considering the fact that the actual impact velocity is smaller than the initial velocity used for the calculations, the K values are effectively shifted to lower values of Re , moving them even further away from the splashing boundary. Therefore it can be concluded that none of the investigated liquids would splash under the experimental conditions.

Weber and Ohnesorge number can also provide information about the spreading dynamics on the substrate after drop impact. Schiaffino used dimensionless numbers to create an impact regime map to combine his theoretical considerations about spreading. The We number determines the driving force for spreading, whereas the Oh number represents the force that resists spreading [47].

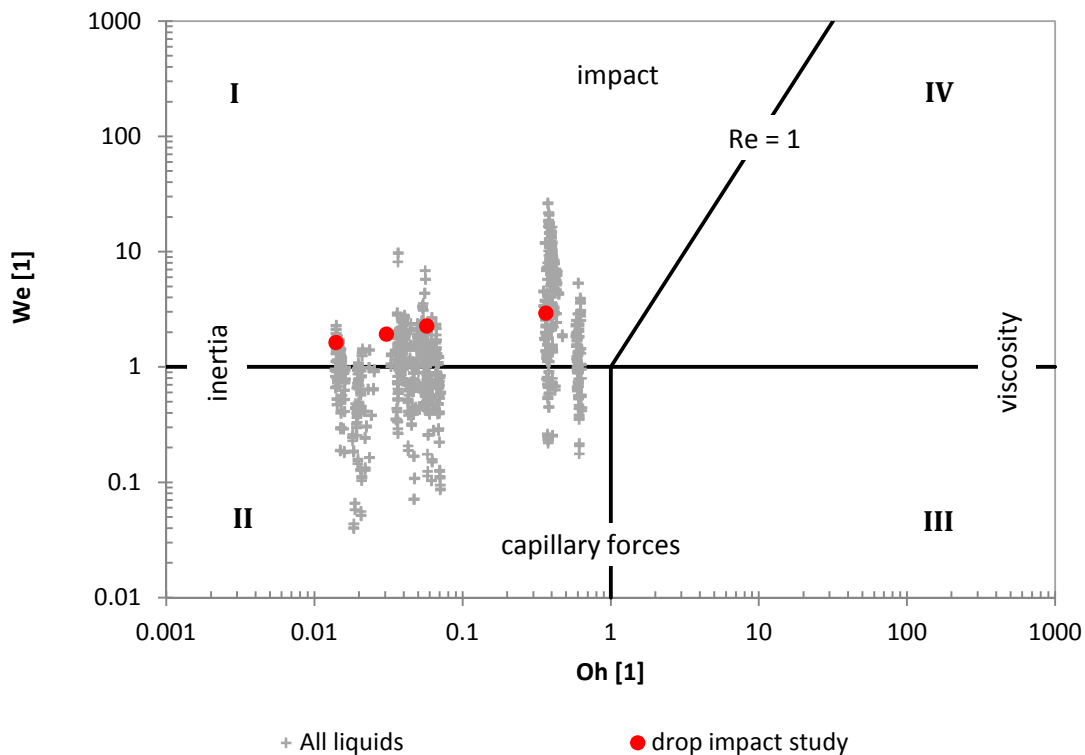


Figure 33: Operational regime map as proposed by [47].

Figure 33 displays the We - Oh plane, which is divided into four spreading regions governed by different forces. The boundary lines are represented by $We = 1$ and $Oh = 1$ for $We \leq 1$, as well as $Re = 1$ for $We > 1$. The gray data points shown in this graph again represent all drop formation measurements, whereas the red points refer explicitly to the drop impact study. All data points are found in either region I or II which means that, while droplet spreading

can be driven by both impact and capillary forces, it is resisted only by inertia. Similar results were also reported by Lim et al. [48] who investigated the spreading of inkjet printed micro droplets on heated substrates.

5.6 DISSOLUTION TESTING

This section is dedicated to the investigation of vitamin release from handmade paper substrates. Dissolution testing is a very common method in drug development to provide information about the solubility and bioavailability of APIs [49].

In general, dissolution tests are performed in various fluids, ranging from water to complex dissolution media that specifically mimic intestinal fluids. In the present case, the dissolution medium of choice was 0.1 M HCl, which simulates the low gastric pH. Usually this is the first physiological environment an API encounters. Table 14 provides a summary of the experimental conditions.

| Liquid | Substrate | Operating parameters |
|--------------------------------|--------------------------------------|----------------------|
| B12 in PG/H ₂ O:3/1 | CaCO ₃ / TiO ₂ | 1000 Hz/115 V/30 μs |
| FA Sus 10 | CaCO ₃ | 1000 Hz/90 V/26 μs |
| FA in 1 M NaOH | CaCO ₃ | 1000 Hz/103 V/24 μs |

Table 14: Materials and operating parameters for printing test substances on paper.

In this study, dissolution testing is primarily used to determine whether an inkjet printed pharmaceutical substance is released from its carrier when suspended in liquid or not. Applying this method also allows for determination of the dissolving rate of the API and the achieved dosing accuracy. A certain target amount of API was printed on a paper stripe of defined dimensions using the MD system. The target amount and the corresponding number of droplets are presented in Table 15. Although the burst mode of the droplet generator is capable of ejecting up to 10000 droplets at one dispensing cycle it is impractical to use it for a large number of droplets. Therefore, with the exception of vitamin B12, all substances were printed in continuous mode. Knowing the dispensing frequency, the right amount of substance was applied by stopping the droplet ejection after a certain time.

| API | Target amount [mg] | Concentration [mg/ml] | Target volume [μ l] | d_d [μ m] | V_d [μ l] | Number of droplets | f [Hz] | t [s] |
|--------|--------------------|-----------------------|--------------------------|------------------|------------------|--------------------|--------|-------|
| B12 | 0.25 | 40 | 6.25 | 79 | 2.58E-04 | 24210 | 1000 | 24 |
| FA-Sus | 5 | 100 | 50.0 | 74 | 2.12E-04 | 235655 | 1000 | 236 |
| Fa-Na | 5 | 180 | 27.8 | 69 | 1.72E-04 | 161492 | 1000 | 161 |

Table 15: Target amounts, API concentration and necessary number of droplets for printing test substances. d_d and V_d correspond to droplet diameter and volume, respectively, f is the dispensing frequency and t the resulting dispensing time.

Consequently, accurate dosing was difficult for several reasons. First of all, the provided operating software was unable to terminate the ejection automatically after a certain time period. Thus, the dispensing time had to be measured using an external timer, and the droplet ejection was controlled manually via a start/stop button. This means that the calculated dispensing time was not precisely met. Furthermore, the applied liquid volume was (especially for FA) too high to be absorbed at once by the paper substrate. Therefore the printing process had to be interrupted to allow the paper to dry before applying more substance. In addition to that, it was impossible to control the droplet size during the printing process itself. To take droplet pictures, the nozzle had to be moved into camera position which was only done when a new paper carrier was inserted. Droplet size was determined by optical measurements, which are, as mentioned in section 5.3, prone to error. Due to overexposure of the images and poor camera resolution, the drop contour is not defined accurately enough to allow for precise diameter and volume calculations. Even small deviations of a few pixels can generate a large difference in droplet volume.

Figure 34 displays the dissolution profiles of vitamin B12 released from CaCO_3 and TiO_2 paper. The dissolved amount of substance is expressed as a percentage of the predetermined target amount. Apparently more than 100% of B12 were released, indicating that the printed amount in fact exceeded the target amount, which can be attributed to the aforementioned dosing difficulties. Vitamin B12 was applied with an ejection rate of 1000 Hz, which should ideally have deposited 1000 droplets per second on the paper substrate. For a mean droplet diameter of 79 μ m, 0.26 μ l B12 solution would be applied per second. Considering that the target amount was only 6.25 μ l, a substance surplus of 4.13% per second would be deposited if the dispensing process is not stopped on time. That means if, for some reason, the dispensing time is exceeded for only two seconds, almost 10% more substance is applied to the substrate.

The graph shows further that the substance dissolved completely within the first 5 minutes of dissolution testing. After that, the concentration remains almost constant.

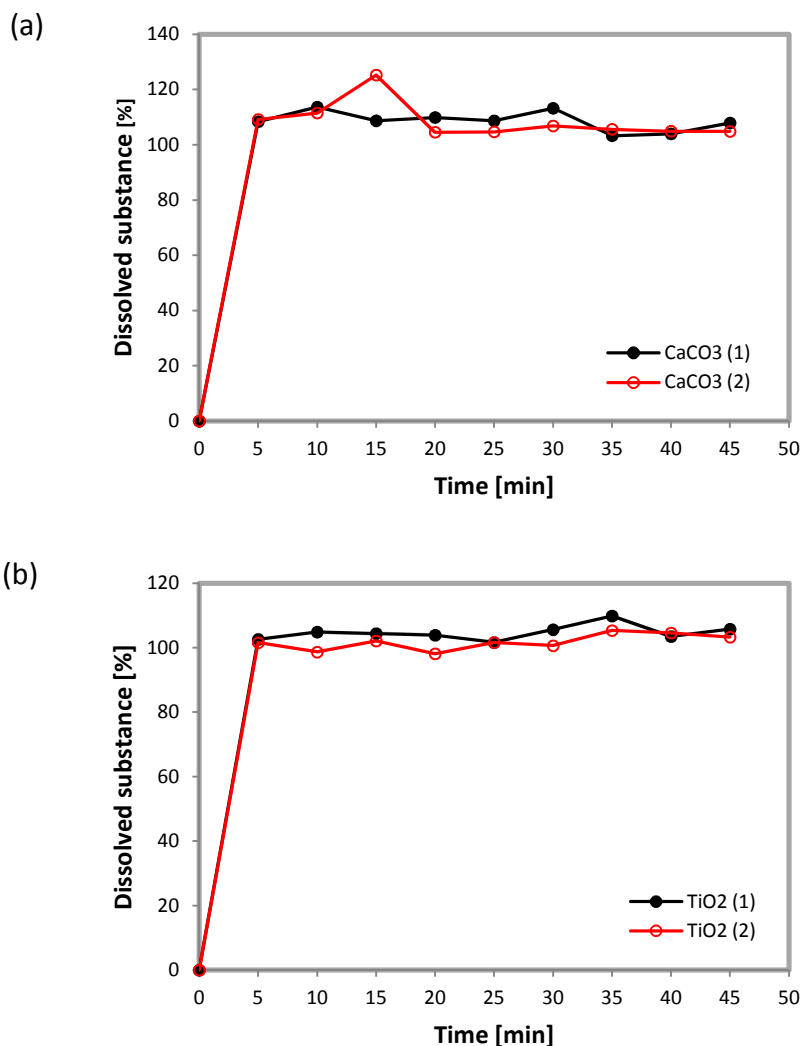


Figure 34: Dissolution profiles of B12 printed on (a) CaCO₃ and (b) TiO₂ paper.

Due to its faster disintegration only, CaCO₃ paper was used in the subsequent experiments. Folic acid showed very slow release due to its poor solubility in acidic environment (figure 35). FA carries two carboxyl groups, which are protonated in acidic environment. Therefore it is more hydrophobic than the deprotonated molecule, and hence less soluble. Since the poorly soluble FA was not released properly from the paper carrier in the first place, it is not possible to draw definite conclusions concerning dosing accuracy from this test. To measure the FA concentration nonetheless, each sample was prepared with 2 M NaOH prior to HPLC analysis to convert the carboxyl groups to carboxylate anions. The slow release profile also indicates that the pure unmodified FA would not be well ingested via the stomach. Similar

results concerning the solubility of FA in simulated gastric fluid were also reported by Younis et al., who investigated the quality of commercially available folic acid supplements [50].

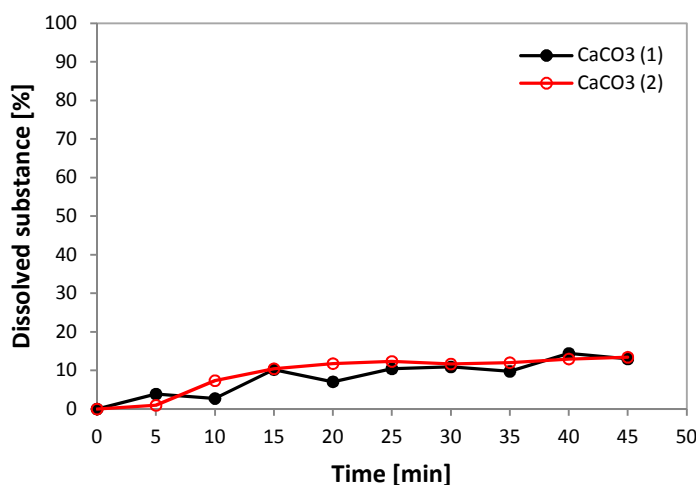


Figure 35: Dissolution profiles of folic acid printed on CaCO₃ paper.

In contrast to untreated FA, sodium folate showed good solubility in aqueous solution. This can probably be attributed to the fact that the two carboxyl groups are already converted to the corresponding anions. The dissolution results of printed Na-folate on CaCO₃ are presented in Figure 36. The graph shows an initial rise, followed by a steady decrease of concentration of the dissolved substance. The highest concentration of folate is found within the first 10 minutes of dissolution. A reason for the steady decline in concentration with time could be a slow back reaction of folate to FA in acidic medium. During dissolution in HCl, folate could be reprotonated to the less soluble acid form. Furthermore, the target dosage of 5 mg was not achieved on sample CaCO₃ (1). The shape of the profiles may indicate that the folate solution was not dosed accurately onto the substrate because the release rate and the subsequent decline appear to be similar to that of sample CaCO₃ (2).

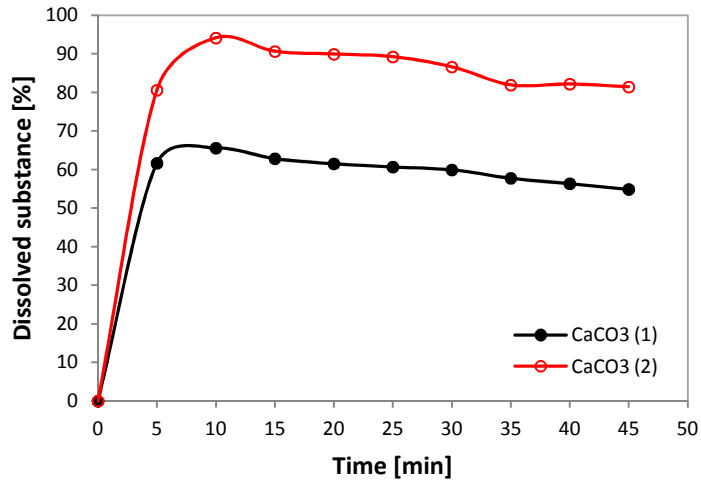


Figure 36: Dissolution profiles of Na-folate solution printed on CaCO₃ paper.

5.7 DIMENSIONAL ANALYSIS AND CORRELATION MODEL

One important aspect of this work was to gain quantitative information about the DOD drop formation process. Section 5.3 already provided an empirical description of microdrop formation. The present section focuses on the determination of scaling laws for the prediction of droplet diameter and velocity immediately after drop formation. These scaling laws allow for calculation of the resulting diameter and velocity for liquids with known physical properties and with the set of operating parameters given, which could be useful for automated dosing of pharmaceutical substances.

After identifying the factors relevant for DOD drop formation, a dimensional analysis was performed according to the method described in section 3.3.2. The quantities affecting the droplet diameter d_d and velocity u are the physical properties of the used liquid, the operating parameters of the droplet generator, the piezoelectric constant of the actuator and the diameter of the capillary. Table 16 lists the two target quantities and their corresponding relevance lists.

| | | Unit | Target quantity | |
|----------------------|------------------------|----------------------|------------------------|---------------------------|
| | | | Drop diameter d_d | Drop velocity u |
| Liquid properties | Density | [kg/m ³] | ρ | ρ |
| | Dynamic viscosity | [Pas] | μ | μ |
| | Surface tension | [N/m] | σ | σ |
| Operation parameters | Voltage amplitude | [V] | ΔU | $(\Delta U - \Delta U^*)$ |
| | Frequency | [s ⁻¹] | f | f |
| | Pulse width | [s] | τ | τ |
| Actuator constants | Piezoelectric constant | [m/v] | β | β |
| | Capillary diameter | [m] | d | d |

Table 16: Relevance lists for the target quantities drop diameter and velocity. For the drop velocity, the voltage amplitude was replaced by the term $(\Delta U - \Delta U^*)$ with the threshold ΔU^* of the signal amplitude, which was experimentally determined. $\beta = 3 \cdot 10^{-10}$ m/V; $d = 800$ μ m.

Since only one droplet generator with a fixed capillary diameter d was available for all drop formation experiments, information concerning the influence of this parameter on drop formation cannot be provided at this point. The above stated piezoelectric constant β was taken from a datasheet of a comparable PZT material. Therefore, both d and β serve as constant scaling factors. Because the relevant quantities for both target quantities are similar, five non-dimensional groups were found by the dimensional analysis for each of them. The resulting relations for drop diameter and velocity are presented in eq. (6) and eq. (7), respectively.

$$\frac{d_d \mu f}{\sigma} = A \cdot \left(\frac{d \mu f}{\sigma}\right)^{a_1} \cdot \left(\frac{\beta \Delta U}{d}\right)^{a_2} \cdot \left(\frac{\mu}{\sqrt{\rho \sigma d}}\right)^{a_3} \cdot (f \tau)^{a_4} \quad (6)$$

$$\frac{\beta(\Delta U - \Delta U^*) \rho u}{\mu} = B \cdot \left(\frac{\beta(\Delta U - \Delta U^*)}{d}\right)^{b_1} \cdot \left(\frac{\mu}{\sqrt{\sigma d \rho}}\right)^{b_2} \cdot \left(\frac{f d^2 \rho}{\mu}\right)^{b_3} \cdot (f \tau)^{b_4} \quad (7)$$

The equations represent the drop size as a capillary number and the drop velocity as a Reynolds number. The coefficients (A, B) and the exponents (a_1 through a_4 and b_1 through b_4 , respectively) in the equations above were calculated using Microsoft Excel. Since Excel did not offer a suitable non-linear regression function, the equations were logarithmized and subsequently fitted to the experimental data with a linear regression function (LINEST). The resulting scaling laws are presented in the following sections.

5.7.1 CORRELATION FOR THE DROP DIAMETER

In order to describe the droplet size, the liquids listed in table 17 were investigated. The data base includes a wide range of liquid types, i.e. pure solvents, solvent mixtures, particle free vitamin solutions, a vitamin suspension, as well as a short polymer in aqueous solution.

| Liquid | Concentration | |
|-----------------------------------|---------------|------|
| | [mg/ml] | [%] |
| H ₂ O de-ion. | - | - |
| EtOH | - | 99.9 |
| i-PrOH | - | 99.9 |
| H ₂ O/EtOH:7/3 | - | - |
| PG/H ₂ O:3/1 | - | - |
| B12 in H ₂ O/EtOH:7/3 | 40 | 4 |
| B12 in EtOH/H ₂ O:7/3 | 20 | 2 |
| B12 in PG/H ₂ O:3/1 | 40 | 4 |
| B12 in PG/EtOH:3/1 | 40 | 4 |
| FA in 1M NaOH | 180 | 18 |
| B6 in H ₂ O | 180 | 18 |
| 5% wt PEG 300 in H ₂ O | 50 | 5 |
| FA-Sus (1% wt FA, 2% wt T20) | 10 | 1 |

Table 17: Liquids investigated for diameter correlation model.

Based on relation shown in eq. (6) the following equation was found to be the best fit.

$$\frac{d_d \mu_f}{\sigma} = 15.39 \cdot \left(\frac{d \mu_f}{\sigma}\right)^{0.6205} \cdot \left(\frac{\beta \Delta U}{d}\right)^{0.3035} \cdot \left(\frac{\mu}{\sqrt{\rho \sigma d}}\right)^{0.4431} \cdot (f\tau)^{0.3823} \quad (8)$$

The comparison of the measured and the calculated dimensionless droplet diameter is illustrated in figure 37. In case of complete agreement between experiment and model description, all data points would be aligned straight along the red diagonal line. Calculation and experimental data show a very good correlation, as can also be deduced from the high R² value close to 1. Consequently, the droplet diameter can be predicted accurately for liquids with fluid properties similar to those of the test liquids.

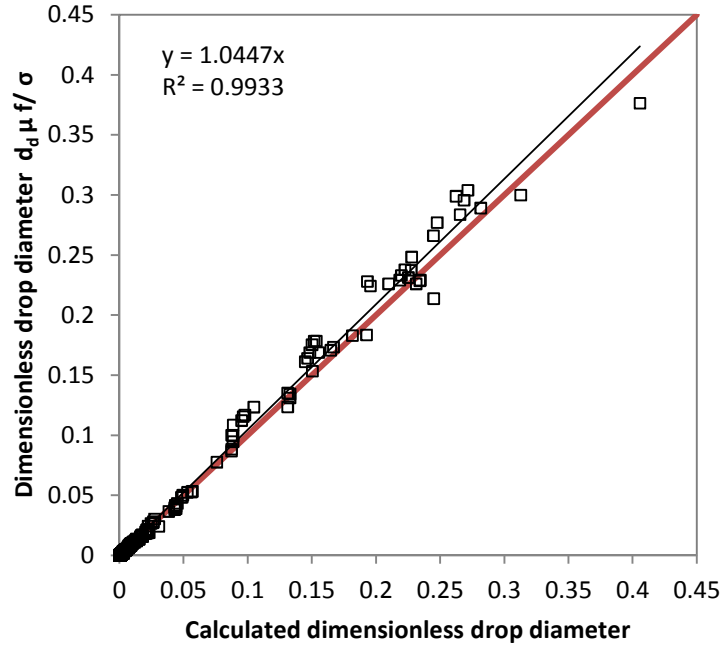


Figure 37: Comparison of dimensionless droplet diameter as measured and calculated by eq. (8).

5.7.2 CORRELATION FOR THE DROP VELOCITY

The data base used for the droplet velocity model was considerably smaller than for the diameter model. 4 liquids (EtOH, 48% wt glycerol in H₂O, PG/H₂O:3/1 and PG/H₂O:1/1) with different fluid properties were chosen to provide sufficient data for a correlation. In drop formation experiments (see section 5.3) the dependency of drop size and velocity on the operating parameters (actuator frequency f , actuation voltage ΔU and pulse width τ) was investigated. The results of these experiments are shown in figure 26 and figure 27. A threshold voltage ΔU^* derived from the actuation voltage experiment (figure 27c) represents the minimum actuation voltage necessary to eject a droplet from the nozzle. Thus the actuation voltage ΔU is replaced with the excess voltage $(\Delta U - \Delta U^*)$, because only the excess voltage is relevant to producing droplet velocities greater than zero. Eq. (9) shows the scaling law for droplet velocity determined from fitting drop formation data to eq. (7) .

$$\frac{\beta(\Delta U - \Delta U^*)\rho u}{\mu} = 2.341 \cdot 10^5 \cdot \left(\frac{\beta(\Delta U - \Delta U^*)}{d}\right)^{2.065} \cdot \left(\frac{\mu}{\sqrt{\sigma d \rho}}\right)^{0.271} \cdot \left(\frac{f d^2 \rho}{\mu}\right)^{1.399} \cdot (f\tau)^{-0.531} \quad (9)$$

Only data obtained from measurements at a constant actuation frequency of 100 Hz was used for this correlation. The threshold voltages were derived from measurements at 100

Hz, and a dependency of the threshold voltage from the frequency cannot be excluded at this point.

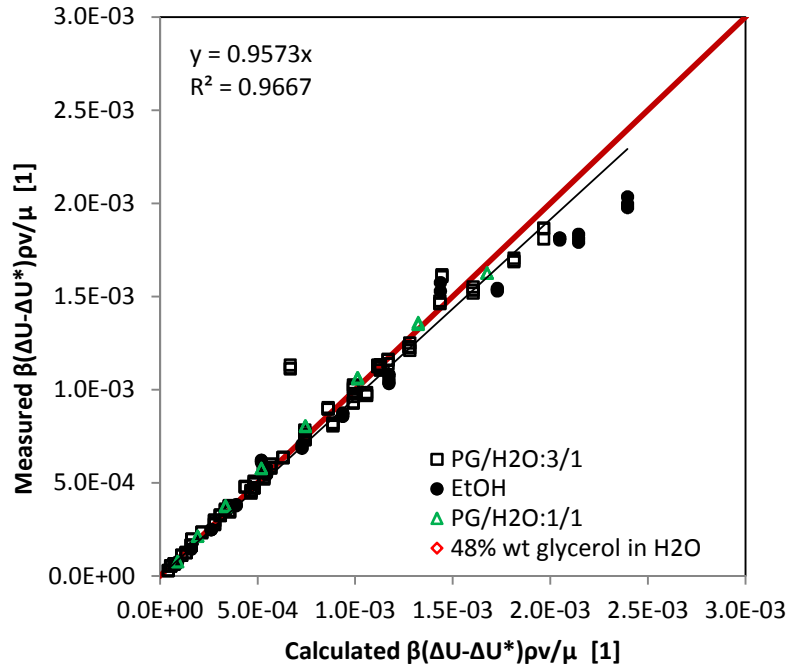


Figure 38: Comparison of dimensionless droplet velocity as measured and calculated.

In figure 38 the dimensionless droplet velocity derived from measurements is compared to the velocity calculated from eq. (9). The red diagonal line indicates complete agreement of calculated and measured data. As can be seen from the graph, the agreement is good which is also indicated by the R^2 value close to 1. This means that the experimental data is well represented by the scaling law.

6 SUMMARY AND CONCLUSIONS

Inkjet printing is one of the most versatile methods to deposit liquids on a wide range of substrates. The highly reproducible dispensing and precise placement of microdroplets, and the fact that inkjet printing is a noncontact method, are just some of the key benefits of this technology.

This study represents an attempt to develop inkjet printing as a method to apply pharmaceutical substances on edible paper substrates for the preparation of individualized low dosage forms. A summary of the main findings of this work as well as some concluding remarks are presented in the following sections.

6.1 SUMMARY

Liquid formulations of three vitamins (B6, B12 and FA) were successfully prepared in the form of solutions or suspensions. Density, surface tension, dynamic viscosity and the equilibrium contact angle against glass were determined for each liquid. Rheological experiments showed that, within a shear rate range of $1 - 100\text{s}^{-1}$, all tested liquids were Newtonian. Ejectable liquid formulations were only found for B12 and FA. B6 dissolved in H_2O tended to recrystallisation in the glass capillary of the droplet dispenser and could therefore not be ejected with sufficient reliability. The addition of PG to a B6 solution improved ejection performance. However, the B6 solution did still not produce monodisperse droplets in every experiment.

The generation of monodisperse droplets with coating fluids was only successful for diluted polymer solutions (1% - 1.5% wt). Liquids with higher polymer content were either too viscous to be jetted or led immediately to clogging of the dispenser nozzle. FA suspensions with a particle content ranging from 1 to 20% wt were also tested for their jetting properties. Best results were achieved with a suspension containing 10% wt FA and 3% wt T20 as a stabilizing agent.

Based on their ejectability, the tested liquids were categorized into three regions on a graph displaying dynamic viscosity vs. surface tension. A dynamic viscosity between 20 and 30 mPas and a surface tension between 30 and 40 mN/m were found to be ideally suited for this particular dispensing system. Since fluids with both low and high density were found to be reliably ejectable, the influence of density remains an open question.

In addition, the different stages of drop formation were visualized and discussed in terms of their liquid properties. Drop diameter and velocity were investigated as functions of the applied operating parameters (dispensing frequency, pulse width and pulse amplitude). The drop diameter increased with increasing pulse width and amplitude, the drop velocity increased significantly with the driving amplitude. The influence of the actuation frequency, however, was not as obvious and requires therefore a more in depth investigation.

The accuracy of the dispensing process was investigated by weighing liquid portions that were dispensed either in bursts of 100, 1000 and 10000 droplets or continuously for 2 minutes using a highly sensitive balance. The droplet mass derived from the gravimetric experiments was then compared to optical measurements. The droplet mass determined by weighing was higher than the mass calculated from drop imaged. Furthermore, the droplet ejection in continuous mode showed better reproducibility than in burst mode. The variation in droplet mass was dependent on the liquid amount dispensed in one burst and increased with decreasing number of droplets.

The drop impact tests on glass and four paper substrates showed complete deposition of all droplets. The experimental data was compared to a correlation found by Mundo et al. [38] that confirmed further that the impact velocity for all tested liquids was too small to cause droplet splashing upon impact.

Dissolution profiles indicated that the release from the paper carrier was fast and complete within the first five minutes for all test substances with the exception of nanodispersed folic acid which is hardly soluble in the used test medium.

There was no significant difference in release between TiO_2 and CaCO_3 paper, but CaCO_3 paper disintegrated faster in acidic solution. In the case of vitamin B12, the released amount exceeded the target amount which was probably caused by dosing difficulties.

Correlation models to predict droplet size and velocity were derived from experimental data. The correlations were good for both models with R^2 values of 0.9933 and 0.9667 for diameter and velocity, respectively.

6.2 CONCLUDING REMARKS

To better investigate the ejection properties of future test liquids, rheological measurements should be repeated at constant temperature within a shear rate range of $1\text{-}1000\text{s}^{-1}$. Although

shear rates can be much higher in DOD inkjet capillaries, this is usually considered as sufficient to assess the ejectability of a liquid [40][12].

Since fluids with higher viscosity showed better ejection performance, I would recommend exploring more mixtures of high viscosity, pharmaceutically applicable liquids like glycerol, PEG 300 and PG. These liquids could improve the printing process for many substances, because they not only act as viscosity modifiers, but also as humectants which prevent the evaporation of the primary solvent, and thus potential clogging of the nozzle [14]. Furthermore, it should be taken into consideration to use API derivatives with enhanced solubility to avoid that the liquid capacity of the paper carrier is exceeded.

The printing of polymeric solutions using a DOD inkjet system has been successfully applied in other fields [8][51][52]. However, printing of protective Eudragit coatings on porous substrates proved to be unsuccessful. While it was possible to eject highly diluted polymer solutions, the drop formation process was very unreliable. Process downtimes led usually to clogging of the printhead which required cleaning with harsh chemicals that potentially damage the glass capillary. Moreover, the solvent of the coating solution could partly dissolve the applied API and cause it to elute from the very thin paper carrier. Therefore, I would recommend precoating the paper substrate with a protective film on one side of the paper using a different coating technique and applying a second layer of coating on top of the deposited API.

To obtain more information about the influence of the nozzle diameter on drop formation, it would be helpful to repeat the measurements using droplet generators with different nozzle diameters.

The study was confined to the application of a rectangular driving signal waveform determined by the used equipment. It would be interesting to investigate other driving signals, like a double pulse or bipolar pulse excitation. This could not only improve the ejection performance of problematic test fluids with a strong tendency to form a spray or satellite droplets, but also allow for the production of even smaller droplets with the same nozzle diameter [14][53].

Another issue that necessitates further work is the dispensing accuracy of the applied DOD system. In order to meet the goal to dispense liquids with high accuracy, the optical measurement has to be dramatically improved. To obtain images that allow for a sufficiently precise determination of the droplet diameter, it is necessary to use a camera with higher

geometric and radiometric resolution. The current equipment does not provide that level of accuracy because it was designed to observe the droplet deposition on the substrate, but not to provide images to calculate the droplet size. It is further recommended to use an aperture to ensure that the resulting images are not overexposed. Also, a more evenly illuminated background on droplet images could improve the calculations. In addition, the software determining the droplet contour line could get better results if the region of interest was determined first and the threshold after that.

Finally, it would be helpful if the control system of the sample stage was integrated with the printhead into one program, so that the complete process could be automated.

Many interesting questions still remain unanswered. For example, it would be of further interest to study interactions between the paper carrier and the API. Also, due to time limitations, the application of multiple APIs on the same substrate was not conducted. Although some difficulties and limitations were encountered, it would be rash to conclude that inkjet printing is not suitable for the intended purpose. I hope, however, that the results presented in this work are a starting point for future investigations.

7 REFERENCES

- [1] A. Bruns, H. Hoffelner and J. Overmann, "A novel approach for high throughput cultivation assays and the isolation of planktonic bacteria," *FEMS Microbiology Ecology*, vol. 45, pp. 161-171, 2003.
- [2] O. Gutmann, R. Niekrawietz, R. Kuehlewein, C. P. Steinert, B. de Heij, R. Zengerle and M. Daub, "Impact of medium properties on droplet release in a highly parallel nanoliter dispenser," *Sensors and Actuators A*, vol. 116, pp. 187-194, 2004.
- [3] A. Schober, R. Günther, A. Schwienhorst, M. Döring and B. F. Lindemann, "Accurate high-speed liquid handling of very small biological samples," *Biotechniques*, vol. 15, pp. 324-329, 1993.
- [4] R. E. Saunders, J. E. Gough and B. Derby, "Delivery of human fibroblast cells by piezoelectric drop-on-demand inkjet printing," *Biomaterials*, vol. 29, pp. 193-203, 2008.
- [5] M. Englmann, A. Fekete, I. Gebefügi and P. Schmitt-Kopplin, "The dosage of small volumes for chromatographic quantifications using a drop-on-demand dispenser system," *Analytical and Bioanalytical Chemistry*, vol. 388, pp. 1109-1116, 2007.
- [6] U. Weierstall, R. B. Doak, J. C. H. Spence, D. Starodub, D. Shapiro, P. Kennedy, J. Warner, G. G. Hembree, P. Fromme and H. N. Chapman, "Droplet streams for serial crystallography of proteins," *Experiments in Fluids*, vol. 44, pp. 675-689, 2008.
- [7] J. Dijkman, P. C. Duineveld, M. J. J. Hack, A. Pierik, J. Rensen, J.-E. Rubingh, I. S. Schram and M. M. Vernhout, "Precision ink jet printing of polymer light emitting displays," *Journal of Materials Chemistry*, vol. 17, pp. 511-522, 2007.
- [8] B.-J. de Gans and U. S. Schubert, "Inkjet Printing of Polymer Micro-Arrays and Libraries: Instrumentation, Requirements, and Perspectives," *Macromolecular Rapid Communications*, vol. 24, pp. 659-666, 2003.

- [9] K.-C. Fan, J.-Y. Chen, C.-H. Wang and W.-C. Pan, "Development of a drop-on-demand droplet generator for one-drop-fill technology," *Sensors and Actuators A: Physical*, vol. 147, pp. 649-655, 2008.
- [10] E. Özkol, J. Ebert and R. Telle, "An experimental analysis of the influence of the ink properties on the drop formation for direct thermal inkjet printing of high solid content aqueous 3Y-TZP suspensions," *Journal of the European Ceramic Society*, vol. 30, pp. 1669-1678, 2010.
- [11] N. Reis, C. Ainsley and B. Derby, "Ink-Jet delivery of particle suspensions by piezoelectric droplet ejectors," *Journal of Applied Physics*, vol. 97, pp. 0949031-0949036, 2005.
- [12] K. A. M. Seerden, N. Reis, J. R. G. Evans, P. S. Grant, J. W. Halloran and B. Derby, "Ink-Jet Printing of Wax-Based Alumina Suspensions," *Journal of the American Ceramic Society*, vol. 84, pp. 2514-2520, 2001.
- [13] M. Tsai, W. Hwang, H. Chou and P. Hsieh, "Effects of pulse voltage on inkjet printing of a silver nanopowder suspension," *Nanotechnology*, vol. 19, pp. 3353041-3353049, 2008.
- [14] E. R. Lee, *Microdrop Generation*, S. E. Lyshevski, Ed., Boca Raton: CRC Press LLC, 2003.
- [15] D. B. Bogy and F. E. Talke, "Experimental and Theoretical Study of Wave Propagation Phenomena in Drop-on-Demand Ink Jet Devices," *IBM Journal of Research and Development*, vol. 28, pp. 314-321, 1984.
- [16] J. T. Rubino, "Cosolvents and Cosolvency," in *Encyclopedia of Pharmaceutical Technology*, J. Swarbrick, Ed., New York, Informa Healthcare USA, Inc., 2007, pp. 806-819.
- [17] M. D. Croucher and M. L. Hair, "Design Criteria and Future Directions in Inkjet Ink Technology," *Industrial & Engineering Chemistry Research*, vol. 28, pp. 1712-1718, 1989.
- [18] B. Elvers, Ed., "Vitamins," in *Ullmann's Encyclopedia of Industrial Chemistry*, Weinheim, Wiley-VCH GmbH & Co.KGaA, 2005.

- [19] Z. Wu, X. Li, C. Hou and Y. Qian, "Solubility of Folic Acid in Water at pH Values between 0 and 7 at Temperatures (298.15, 303.15, and 313.15) K," *Journal of Chemical and Engineering Data*, vol. 55, pp. 3958-3961, 2010.
- [20] "RÖMPP Online," Thieme Chemistry, 26 September 2012. [Online]. Available: <http://www.roempp.com>. [Accessed October 2012].
- [21] B. Saidi and J. J. Warthesen, "Influence of pH and Light on the Kinetics of Vitamin B6 Degradation," *Journal of Agricultural and Food Chemistry*, vol. 31, pp. 876-880, 1983.
- [22] M. Hochberg, D. Melnick and B. L. Oser, "On the stability of pyridoxine," *Journal of Biological Chemistry*, vol. 155, pp. 129-136, 1944.
- [23] A. R. Biamonte and G. H. Schneller, "A Study of Folic Acid Stability in Solutions of the B-Complex Vitamins," *Journal of the American Pharmaceutical Association*, vol. 40, pp. 313-320, 1951.
- [24] S. Scheindlin, A. Lee and I. Griffith, "The Action of Riboflavin on Folic Acid," *Journal of the American Pharmaceutical Association*, vol. 41, pp. 420-427, 1952.
- [25] R. P. Tansey and G. H. Schneller, "Studies in the Stabilization of Folic Acid in Liquid Pharmaceutical Preparations," *Journal of the American Pharmaceutical Association*, vol. 44, pp. 34-37, 1955.
- [26] M. J. Akhtar, M. A. Khan and I. Ahmad, "Effect of riboflavin on the photolysis of folic acid in aqueous solution," *Journal of Pharmaceutical and Biomedical Analysis*, vol. 23, pp. 1039-1044, 2000.
- [27] M. J. Akhtar, M. A. Khan and I. Ahmad, "Identification of photoproducts of folic acid and its degradation pathways in aqueous solution," *Journal of Pharmaceutical and Biomedical Analysis*, vol. 31, pp. 579-588, 2003.
- [28] W. L. C. Veer, J. H. Edelhausen, H. G. Wijmenga and J. Lens, "The relation between Vitamins B12 and B12b," *Biochimica et Biophysica Acta*, vol. 6, pp. 225-228, 1950.

- [29] L. J. DeMerre and C. Wilson, "Photolysis of Vitamin B12," *Journal of the American Pharmaceutical Association*, vol. 45, pp. 129-134, 1956.
- [30] I. Ahmad, W. Hussain and A. A. Fareedi, "Photolysis of cyanocobalamin in aqueous solution," *Journal of Pharmaceutical and Biomedical Analysis*, vol. 10, pp. 9-15, 1992.
- [31] L. A. Felton, "Film Coating of Oral Solid Dosage Forms," in *Encyclopedia of Pharmaceutical Technology*, J. Swarbrick, Ed., New York, Informa Healthcare USA, Inc., 2007, pp. 1729-1747.
- [32] R. C. Rowe, P. J. Sheskey and S. C. Owen, Eds., *Handbook of Pharmaceutical Excipients*, 5 ed., London: Pharmaceutical Press, American Pharmacists Association, 2006.
- [33] H. Dong and W. W. Carr, "An experimental study of drop-on-demand drop formation," *Physics of Fluids*, vol. 18, pp. 0721021-07210216, 2006.
- [34] M. Zlokarnik, *Dimensional Analysis and Scale-up in Chemical Engineering*, Berlin: Springer, 1991.
- [35] R. M. Verkouteren and J. R. Verkouteren, "Inkjet Metrology: High-Accuracy Mass Measurements of Microdroplets Produced by a Drop-on-Demand dispenser," *Analytical Chemistry*, vol. 81, pp. 8577-8584, 2009.
- [36] O. Heudi, T. Kiliç and P. Fontannaz, "Separation of water-soluble vitamins by reversed-phase high performance liquid chromatography with ultra-violet detection: Application to polyvitaminated premixes," *Journal of Chromatography A*, vol. 1070, pp. 49-56, 2005.
- [37] C. Pilz and G. Brenn, "On the critical bubble volume at the rise velocity jump," *Journal of Non-Newtonian Fluid Mechanics*, vol. 145, pp. 124-138, 2007.
- [38] C. Mundo, M. Sommerfeld and C. Tropea, "Droplet-wall collisions: Experimental studies of the deformation and breakup process," *International Journal of Multiphase Flow*, vol. 21, pp. 151-173, 1995.

- [39] C. D. Stow and M. G. Hadfield, "An experimental investigation of fluid flow resulting from the impact of a water drop with an unyielding dry surface," *Proceedings of the Royal Society London A*, vol. 373, pp. 419-441, 1981.
- [40] R. M. Meixner, D. Cibis, K. Krueger and H. Goebel, "Characterization of polymer inks for drop-on-demand printing systems," *Microsystem Technologies*, vol. 14, pp. 1137-1142, 2008.
- [41] K. Holmberg, B. Jönsson, B. Kronberg and B. Lindman, *Surfactants and Polymers in Aqueous Solution*, Chichester: John Wiley & Sons Ltd., 2002.
- [42] D. Myers, *Surfaces, Interfaces and Colloids*, 2nd ed., New York: John Wiley & Sons Inc., 1999.
- [43] K. O. R. Lehmann, "Chemistry and Application Properties of Polymethacrylate Coating Systems," in *Aqueous Polymeric Coatings for Pharmaceutical Dosage Forms*, 2 ed., J. W. McGinity, Ed., New York, Marcel Dekker Inc., 1997.
- [44] J. Pardeike, D. M. Strohmeier, N. Schrödl, C. Voura, M. Gruber, J. G. Khinast and A. Zimmer, "Nanosuspensions as advanced printing ink for accurate dosing of poorly soluble drugs in personalized medicines," *International Journal of Pharmaceutics*, vol. 420, pp. 93-100, 2011.
- [45] V. A. M. Dorfner, "Einfluß der Flüssigkeitseigenschaften auf den Zerfall eines Flüssigkeitsfilms und die resultierenden Tropfengrößen," Ph.D. thesis, Friedrich-Alexander University Erlangen-Nürnberg, Germany, 1994.
- [46] T. Krüger, K. Thurow and N. Stoll, "Optische Volumenbestimmung für die Dosierung kleinster Volumina," *Technisches Messen*, vol. 76, pp. 8-15, 2009.
- [47] S. Schiaffino, "The fundamentals of molten microdrop deposition and solidification," Ph.D thesis, Massachusetts Institute of Technology, Cambridge, MA, 1996.

- [48] T. Lim, S. Han, J. Chung, J. T. Chung, S. Ko and C. P. Grigoropoulos, "Experimental study on spreading and evaporation of inkjet printed pico-liter droplet on a heated substrate," *International Journal of Heat and Mass Transfer*, vol. 52, pp. 431-441, 2009.
- [49] A. M. Dyas and U. U. Shah, "Dissolution and Dissolution Testing," in *Encyclopedia of Pharmaceutical Technology*, J. Swarbrick, Ed., New York, Informa Healthcare USA Inc., 2007, pp. 908-928.
- [50] I. R. Younis, M. K. Stamatakis, P. S. Callery and P. J. Meyer-Stout, "Influence of pH on the dissolution of folic acid supplements," *International Journal of Pharmaceutics*, vol. 367, pp. 97-102, 2009.
- [51] E. Tekin, B.-J. de Gans and U. S. Schubert, "Ink-jet printing of polymers - from single dots to thin film libraries," *Journal of Materials Chemistry*, vol. 14, pp. 2627-2632, 2004.
- [52] V. Fakhfour, G. Mermoud, J. Y. Kim, A. Martinoli and J. Brugger, "Drop-On-Demand Inkjet Printing of SU-8 Polymer," *Micro and Nanosystems*, vol. 1, pp. 63-67, 2009.
- [53] H. Y. Gan, X. Shan, T. Eriksson, B. K. Lok and Y. C. Lam, "Reduction of droplet volume by controlling actuating waveforms in inkjet printing for micro-pattern formation," *Journal of Micromechanics and Microengineering*, vol. 19, pp. 0550101-0550108, 2009.